

From the Division of Neurogeriatrics
Department of Neurobiology, Care Sciences and Society
Karolinska Institutet, Stockholm, Sweden

MOLECULAR BASIS FOR CHAPERONE ACTIVITIES OF THE BRICHOS DOMAIN AGAINST DIFFERENT TYPES OF CLUMPY CLIENTS – A ROUTE TO PREVENT AMYLOID TOXICITY

Axel Leppert



**Karolinska
Institutet**

Stockholm 2020

Cover: Painting named “Bricolore” by Jessica Bunz

All previously published papers were reproduced with permission from the publisher.

Published by Karolinska Institutet.

Printed by Universitetservice, US-AB

© Axel Leppert, 2020

ISBN 978-91-7831-938-1

Molecular basis for chaperone activities of the BRICHOS domain against different types of clumpy clients – a route to prevent amyloid toxicity

Thesis for doctoral degree (Ph.D.)

Public defense: Friday 11th of December at 14:00

Erna Möllersalen, Neo, floor 5, Blickagången 16, 141 52 Huddinge

By

Axel Leppert

Principal Supervisor:

Prof. Jan Johansson, Ph.D.
Karolinska Institutet
Department of Neurobiology,
Care Sciences and Society
Division of Neurogeriatrics,
and Department of Bionut

Co-supervisor(s):

Henrik Biverstål, Ph.D.
Karolinska Institutet
Department of Neurobiology,
Care Sciences and Society
Division of Neurogeriatrics,
and Department of Bionut

Jenny Presto, Ph.D.

Karolinska Institutet
Department of Neurobiology,
Care Sciences and Society
Division of Neurogeriatrics,
and Department of Bionut

Opponent:

Prof. Ursula Jakob, Ph.D.
University of Michigan
Department of Biological Chemistry

Examination Board:

Prof. Pär Nordlund, Ph.D.
Karolinska Institutet
Department of Oncology-Pathology

Assoc. Prof. Claes Andréasson, Ph.D.
Stockholms Universitet
Department of Molecular Biosciences

Assoc. Prof. Elin Esbjörner Winters, Ph.D.
Chalmers Tekniska Högskola
Department of Biology and Biological Engineering

“Aller Unfug ist schwer.” – (Lebensmotto von Otto Walkes)

ABSTRACT

Protein aggregation is a hallmark of a wide range of human disorders, including Alzheimer's disease and type II diabetes, and are often associated with imbalances in the cellular protein homeostasis. Molecular chaperones play an important role in modulating proteostasis and thereby counteract toxic consequences of misfolded or aggregated proteins. In this thesis, we investigated the molecular chaperone functions of several isolated BRICHOS domains against amyloid fibril formation and non-fibrillar protein aggregation. We propose that the ability of the BRICHOS domain to chaperone substrates with structurally distinct aggregation pathways is encoded in its ability to form different assembly states.

BRICHOS domains are found in about ten distantly related protein families. It was proposed that they have an intramolecular chaperone-like function, preventing misfolding of a β -sheet prone region within their respective precursor proteins. Surprisingly, the activity of the Bri2 BRICHOS and proSP-C BRICHOS domain can extend to other aggregation-prone peptides and proteins. However, the molecular mechanisms of this diverse substrate spectrum remained unclear. Here we show that the Bri2 BRICHOS domain forms polydisperse assembly states ranging from monomers, that efficiently reduce amyloid-associated neurotoxicity in hippocampal mouse brain slices, to large oligomers that exclusively exhibit activities against non-fibrillar protein aggregation (paper I). Based on these findings, we designed a stable Bri2 BRICHOS monomer mutant that specifically blocks the formation of toxic species during amyloid fibril formation and partly disassembles wild-type Bri2 BRICHOS oligomers into monomers (paper II). Furthermore, we show that the conversion from Bri2 BRICHOS monomers towards large oligomers and hence the generation of activities against non-fibrillar protein aggregation is triggered by reducing conditions and is mediated through distinct thiol reactivities (paper III). The ability to adopt polydisperse assembly states together with activities against fibrillar and non-fibrillar protein aggregation are not only limited to Bri2 BRICHOS but similarly apply to Bri3 BRICHOS (paper IV). In contrast to Bri2 BRICHOS and Bri3 BRICHOS, proSP-C BRICHOS exists mostly as trimers in solution but a mutation at the homologous position in Bri2 BRICHOS (as shown in paper II) similarly resulted in a stable proSP-C BRICHOS monomer variant. This monomer mutant enabled us to investigate in detail the binding spectrum of the proSP-C BRICHOS domain towards different aggregates during amyloid fibril formation (paper V).

This thesis gives new insights into the structure and function relationship of the molecular chaperone domain BRICHOS.

LIST OF SCIENTIFIC PAPERS

This doctoral thesis is based on the following original papers, referred to in the text by Roman numerals.

- I. **Bri2 BRICHOS client specificity and chaperone activity are governed by assembly state.**
Chen G., Abelein A., Nilsson H. E., **Leppert A.**, Andrade-Talavera Y., Tambaro S., Hemmingsson L., Roshan F., Landreh M., Biverstål H., Koeck P. J. B., Presto J., Hebert H., Fisahn A. and Johansson J.
Nature Communications. (2017); 8(1):2081.

- II. **Augmentation of Bri2 molecular chaperone activity against amyloid- β reduces neurotoxicity in mouse hippocampus in vitro.**
Chen G., Andrade-Talavera Y., Tambaro S., **Leppert A.**, Nilsson H. E., Zhong X., Landreh M., Nilsson P., Hebert H., Biverstål H., Fisahn A., Abelein A. and Johansson J.
Communications Biology. (2020); 3(1):32.

- III. **Extracellular small heat shock protein like chaperone function generated under reducing conditions.**
Leppert A., Chen G., Lianoudaki D., Zhong X., Landreh M. and Johansson J.
Manuscript

- IV. **Recombinant Bri3 BRICHOS domain is a molecular chaperone with effect against amyloid formation and non-fibrillar protein aggregation.**
Poska H., **Leppert A.**, Tigro H., Zhong X., Kaldmäe M., Nilsson H. E., Hebert H., Chen G. and Johansson J.
Scientific Reports. (2020); 10(1):9817.

- V. **An ATP-independent anti-amyloid molecular chaperone domain binds to small secondary nucleation competent A β aggregates.**
Leppert A., Tiiman A., Kronqvist N., Landreh M., Abelein A., Vukojević V. and Johansson J.
Manuscript

OTHER PAPERS NOT INCLUDED IN THE THESIS

Recombinant BRICHOS chaperone domains delivered to mouse brain parenchyma by focused ultrasound and microbubbles are internalized by hippocampal and cortical neurons.

Galan-Acosta L., Sierra C., **Leppert A.**, Pouliopoulos A. N., Kwon N., Noel R. L., Tambaro S., Presto J., Nilsson P., Konofagou E. E., Johansson J.
Molecular and Cellular Neuroscience. (2020); 105:103498

High intracellular stability of the spidroin N-terminal domain in spite of abundant amyloidogenic segments revealed by in-cell hydrogen/deuterium exchange mass spectrometry.

Kaldmäe M., **Leppert A.**, Chen G., Sarr M., Sahin C., Nordling K., Kronqvist N., Gonzalvo-Ulla M., Fritz N., Abelein A., Laín S., Biverstål H., Jörnvall H., Lane D. P., Rising A., Johansson J. and Landreh M.
The FEBS Journal. (2019); DOI: 10.1111/febs.15169.

BRICHOS: a chaperone with different activities depending on quaternary structure and cellular location?

Leppert A., Chen G. and Johansson J.
Amyloid. (2019); 26(sup1):152-153.

Blood-brain and blood-cerebrospinal fluid passage of BRICHOS domains from two molecular chaperones in mice.

Tambaro S., Galan-Acosta L., **Leppert A.**, Chen G., Biverstål H., Presto J., Nilsson P. and Johansson J.
Journal of Biological Chemistry. (2019); 294(8):2606-2615.

BRICHOS - an anti-amyloid chaperone: evaluation of blood-brain barrier permeability of Bri2 BRICHOS.

Tambaro S., Galan-Acosta L., **Leppert A.**, Presto J. and Johansson J.
Amyloid. (2017); 24(sup1):7-8.

Dissociation of a BRICHOS trimer into monomers leads to increased inhibitory effect on A β 42 fibril formation.

Biverstål H., Dolfe L., Hermansson E., **Leppert A.**, Reifenrath M., Winblad B., Presto J. and Johansson J.
Biochimica et Biophysica Acta. (2015); 1854(8):835-843.

CONTENTS

1	Introduction.....	1
1.1	Protein basics	1
1.1.1	Protein structure.....	1
1.1.2	Protein folding	3
1.1.3	Protein aggregation.....	5
1.1.4	Amyloid	7
1.1.5	Amyloid formation	7
1.2	Protein aggregation disorders	9
1.2.1	Amyloid-associated disorders	10
1.2.2	Non-amyloid-associated disorders	12
1.3	Protein homeostasis	13
1.3.1	Protein quality control	13
1.3.2	Molecular chaperones.....	14
1.3.3	ATP-independent molecular chaperones	15
1.4	The BRICHOS proteins.....	17
1.4.1	Prosurfactant protein-C (proSP-C).....	18
1.4.2	Integral membrane protein 2B (ITM2B) - Bri2	19
1.4.3	Other BRICHOS proteins.....	20
1.5	The BRICHOS domain.....	22
1.5.1	Structure	22
1.5.2	Function	23
2	Aims of the thesis	25
3	Methodology.....	27
3.1	Characterisation of proteins.....	27
3.1.1	Circular dichroism spectroscopy	27
3.1.2	Mass spectrometry	27
3.2	Evaluation of protein-protein interactions.....	29
3.2.1	Fluorescence basics	29
3.2.2	Kinetics of amyloid fibril formation.....	30
3.2.3	Fluorescence correlation spectroscopy.....	33
4	Results and discussion	37
4.1	Assembly-function relationship of BRICHOS domain proteins	37
4.1.1	Quaternary structures.....	37
4.1.2	Effects on protein aggregation and associated toxicity.....	38

4.1.3	Bri2 BRICHOS assembly mechanism	41
4.2	Modulation of the proSP-C BRICHOS and Bri2 BRICHOS assembly state and anti-amyloid activity	44
4.3	ProSP-C BRICHOS as a tool to study amyloid formation.....	45
5	Conclusions and future perspectives	49
6	Acknowledgments.....	51
7	References	55

LIST OF ABBREVIATIONS

AD	Alzheimer's disease
ALS	Amyotrophic lateral sclerosis
Asp	Aspartic acid
A β	Amyloid- β
A β PP	Amyloid- β precursor protein
bis-ANS	4,4'-bis-1-anilinonaphthalene-8-sulfonate
CD	Circular dichroism
CS	Citrate synthase
Cys	Cysteine
FBD	Familial British dementia
FCCS	Fluorescence cross-correlation spectroscopy
FCS	Fluorescence correlation spectroscopy
FDD	Familial Danish dementia
HMW	High molecular weight
ILD	Interstitial lung disease
MS	Mass spectrometry
PN	Proteostasis network
PQCS	Protein quality control system
SOD1	Superoxide dismutase-1
SPR	Surface plasmon resonance
ThT	Thioflavin T
Trx	Thioredoxin

1 INTRODUCTION

1.1 PROTEIN BASICS

Proteins are essential for the smallest self-sustaining unit of life: the cell. They maintain its metabolism and structure, and mediate communication in large cellular networks in extremely dynamic and challenging milieus. To undertake these diverse roles proteins adopt a wide variety of three-dimensional architectures where some structures are more rigid, others possess a certain degree of structural flexibility and some are even unstructured.

Essentially, proteins are linear polymers made up of one type of building blocks – the amino acids. In theory, the 20 common amino acids can be randomly assembled in an indefinite number of combinations and lengths. Indeed, small peptides that consist of only 3 amino acids to large multidomain proteins with about 27,000 amino acids are found in eukaryotes. How many proteins are actually expressed is still under investigation but there are estimations that about 20,000 proteins comprise the human proteome (1). Nevertheless, this number is likely to increase drastically considering variants of the same protein due to alternative splicing, single amino acid polymorphisms, and posttranslational modifications. One feature that all proteins have in common is that they adopt three-dimensional structures that are designed to optimally perform their function.

1.1.1 Protein structure

A hierarchy of structural levels describes the conformation of a protein. The first level of protein organization is the primary structure which is defined by the order of amino acids that are covalently linked via peptide bonds into a linear chain. From the genetic code 20 amino acids are transcribed and translated, and they all (except proline) have the same backbone structure, consisting of an amino group, an α -carbon and a carboxylic acid group. However, their side chains, located at the α -carbon atom differ and determine the chemical properties of each amino acid. The chemical character of the side chains allows to cluster amino acids according to their properties, for example amphipathic, hydrophobic, hydrophilic, charged, non-charged or aromatic. These various chemical identities have a great impact on how amino acid residues are participating in interactions with each other or water molecules and consequently on protein structure, stability and function. Peptide bonds are formed by the amino and carboxyl group of two neighboring amino acids. This bond has partial double-bond character where the three non-hydrogen atoms are co-planar, limiting free rotation of the peptide bond (Figure 1). In contrast, the $N-C_\alpha$ and $C_\alpha-C$ bonds are single bonds that can

rotate freely unless they are sterically hindered, for example by their side chains. This makes proteins quite special polymers since rigid and flexible bonds alternate, limiting the number of possible conformations.

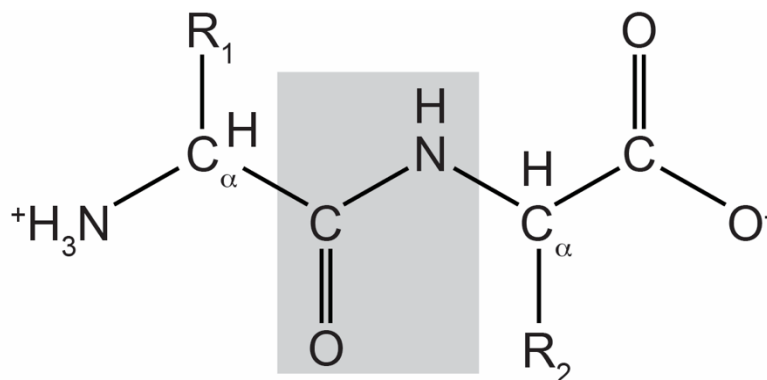


Figure 1: Chemical structure of a dipeptide with the co-planar peptide bond highlighted in grey. The side chains located at the α -carbon atom of the connected amino acids are highlighted with R_1 and R_2 .

Proteins are more than single amino acid residues lined up like pearls on a string but folded three-dimensional entities. The next level of organization is the secondary structure of a protein and describes the local conformation of the polypeptide backbone. It is conceivable that a polymer would exist as random coil but in fact, there are different types of secondary structure elements that are formed by a polypeptide chain: helices, β -sheets, turns, and loops. In general, secondary structure elements are stabilized by regular backbone hydrogen bonds between amino acid residues that are in close proximity. The most common secondary structure element is the α -helix whose shape could be imagined by a winded telephone cord. It is stabilized by hydrogen bonds between the carbonyl oxygen atom of one residue and the amide nitrogen of another residue that is located four residues ahead. The side chains of each amino acid residue project outward from the helix. Contrary to the α -helix, the β -sheet is made of strands that are laterally aligned in a slightly bended plane and held together by hydrogen bonds of the polypeptide backbone. The strands in a β -sheet run parallel or antiparallel but mixed β -sheets with both variants are also found, *e.g.* in the core region of the BRICHOS domain. The strands in the β -sheet can be located in different parts of the polypeptide chain and thereby allow the formation of complex and compact structures.

Even though the secondary structure refers only to the conformation of the peptide backbone, the amino acid side chains at the α -carbon atom influence the structure. For example, long polar residues (arginine, lysine, glutamine, glutamic acid) are more frequently found in α -helices most likely because their side chains can project outward from the helix. On the other

hand, aromatic (tryptophan, tyrosine, phenylalanine) and side chains branched on the β -carbon (valine, isoleucine, threonine) predominate in strands possibly because in a β -sheet every other side chain is pointing in a different direction, allowing the accommodation of bulky side chains or side chains branched close to the polypeptide backbone (2). However, the likelihood of an amino acid occurring in a secondary structure element is also dependent on the local and global environment, neighboring residues, and the final fold of a protein.

Most proteins fold into compact structures that are approximately spherical and therefore referred to as globular. The tertiary structure specifies the final orientation of all unstructured and secondary structure elements of a single polypeptide chain. Nevertheless, long polypeptide chains consist often of two or more domains, that are functional folded subunits with characteristics of individual globular proteins. Furthermore, proteins can assemble into large multimeric complexes made of the same molecule (homomer) or of different molecules (heteromer). This is referred to as the quaternary structure of a protein. The latter two levels of protein organization are strongly influenced by the properties of the amino acid side chains since they contribute to the stability of the fold by electrostatic and hydrophobic interactions, disulfide bridges, Van der Waals contacts and hydrogen bonds (3). In globular proteins, hydrophobic side chains tend to be hidden in the core of a protein or in protein-protein interfaces, while hydrophilic residues locate on the surface. Defining these four levels of protein structure is important to enable a closer look at the processes of how proteins find their correct fold or aggregate under non-favorable conditions.

1.1.2 Protein folding

In the cellular machinery proteins undergo a constant turnover and most of them have half-lives between a few minutes to several hours (4). In order to keep pace with the biochemical reactions in the cell, proteins must adopt their functional three-dimensional structure in a reasonable amount of time. It is astonishing that *in silico* and *in vitro* experiments have shown that some proteins can fold in the low μ s range – at their respective theoretical speed limit (5).

Historically, two main observations paved the way for the field of protein folding. Firstly, Anfinsen and co-workers showed that denatured ribonuclease spontaneously refolds in solution (6) and concluded that all information needed for the native state of a protein is encoded on the primary structure (7). Secondly, Levinthal postulated in 1968 that there is a kinetic paradox regarding the folding speed of proteins. He noted that there is a discrepancy in the folding time of a protein in nature and how long it would theoretically take a denatured

polypeptide chain to refold, if the folding fully depends on a trial and error search of the correct conformation (8). As an example, one could imagine a 100 residues protein, where each amino acid residue of the peptide backbone has one rotational degree of freedom with two possible configurations. This would result in 2^{100} possible conformations and if one assumes a conversion time for each configuration of 1 ps, the time needed to test all combinations to find the correct fold would be far longer than the age of the earth. This illustrates that protein folding cannot work at random and lead to the hypothesis that there are intrinsic properties, that are encoded in the primary structure that guides the polypeptide chain into the correct native conformation (6).

Over the years many theories have emerged to explain the kinetic dilemma of protein folding. One was the framework model, in which secondary structures emerge first in the denatured polypeptide chain, followed by the organization of the pre-formed structures to the native state (9). Another model was the hydrophobic collapse model, where the denatured polypeptide chain collapses, hydrophobic residues are buried in the core and the final fold develops in a restrained volume, thereby limiting the conformational possibilities (10). Even though both models could be experimentally supported under specific conditions they were both lacking explanations for the kinetics and thermodynamics of protein folding. Therefore, a new mechanism was proposed that unites features of both previously mentioned models. In the nucleation-collapse model long range hydrophobic interactions stabilize a folding intermediate with weak secondary structures until the native state is formed (11). Over the years, this view on protein folding was further extended and fine-tuned leading to a funnel-shaped energy landscape of protein folding, illustrated in Figure 2 (12). In theory, many unfolded high energy polypeptide conformations exist that adopt incrementally lower-energy and partially folded intermediates, called molten globule states (13). These meta-stable folds allow exploring of conformations towards the global Gibbs free energy minimum (native state) more rapidly. In this model the unfolded polypeptide chain can take different routes towards the native state and other thermodynamically stable folds may exist. Fast folding proteins may have only a few poorly stable molten globule states and the native state is a deep energy minimum, allowing fast transitions (14). However, complex proteins might have many intermediates that need to overcome energy barriers on their folding pathway as well as convert from several near-native conformations to the correct fold. Therefore, the funnel-shaped energy landscape is often illustrated with valleys (local minima) and hills on the way to the native protein conformation (12, 15). It is also important to mention that the energy landscape looks different for each protein and is highly dependent on the protein environment

and protein-protein interactions. Even though there have been a lot of improvements in the field of protein folding over the years, there are still major difficulties to overcome in order to be able to predict the correct three-dimensional structure of a protein *in silico* (16).

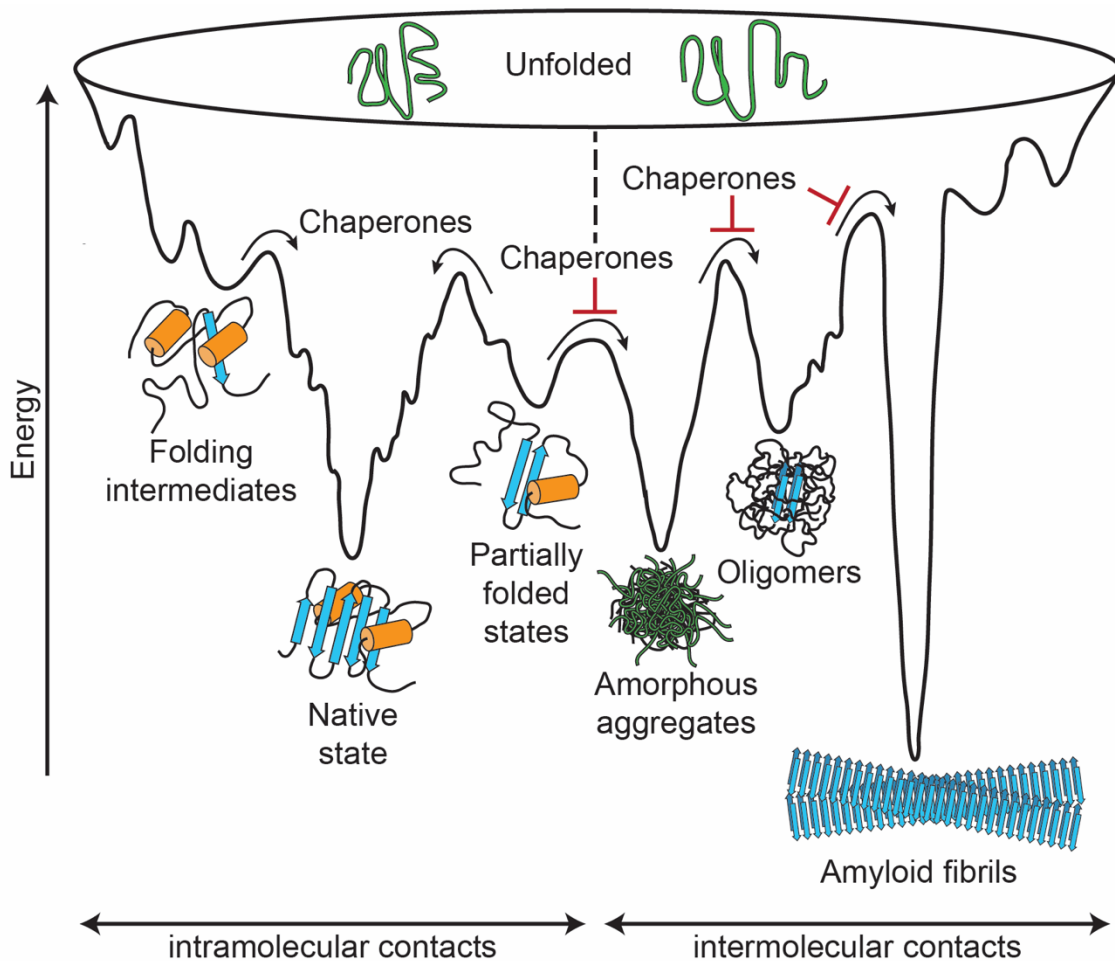


Figure 2: Illustration of the funnel-shaped free energy landscape of protein folding and misfolding, as well as non-fibrillar and fibrillar aggregation. Reproduced from Hartl *et al.* 2011 (17).

1.1.3 Protein aggregation

Protein aggregation is a double-edged sword. On the one hand, protein aggregation is extremely important, for example the main cytoskeletal globular protein actin polymerizes to form filaments, which supply mechanical support to the cell (18). On the other hand, several detrimental human diseases like Alzheimer's disease (AD) or cataract are characterized by protein aggregates of the amyloid- β peptide or crystallin, respectively (19, 20). Non-native protein aggregation involves the formation of large protein assemblies that can be defined in two general categories: amorphous or amyloid. Amorphous aggregation can be understood as the unordered aggregation of proteins in an insoluble structure formed by random

intermolecular contacts. In contrast, amyloid fibrils are highly structured self-assemblies with an ordered cross- β structure (21).

In the literature, protein misfolding and protein aggregation are quite often used interchangeably, but it is important to note that they can be mutually dependent but not necessarily need to be. This becomes clear looking at the origin of large fibrillar aggregates that are formed by the amyloid- β peptide ($A\beta$), found in amyloid plaques in the brains of AD patients. In this case, the aggregate formation is not initiated by a protein that is intrinsically misfolded but instead by processing of the amyloid- β precursor protein ($A\beta$ PP). The precursor protein is folded and inserted into the cell membrane, but aberrant cleavage leads to the production and accumulation of highly aggregation-prone and toxic species. Consequently, AD can be considered as a protein aggregation disorder rather than a protein misfolding disease (22, 23). In contrast, some mutations in superoxide dismutase-1 (SOD1) that are found in familial forms of amyotrophic lateral sclerosis (ALS) destabilize the native protein conformation, thereby increasing non-native self-interactions that lead to the accumulation of insoluble aggregates. In this case, protein misfolding leads to protein aggregation and therefore these SOD1 mutations related to ALS can be considered as protein misfolding diseases (22, 24).

In general, non-native protein conformations have in common that they follow an alternative folding pathway in the energy landscape and if they are not guided back on track, e.g. by molecular chaperones, they can assemble and get trapped in low energy minima as aggregates (Figure 2) (25). Especially, folding intermediates or misfolded proteins are likely to expose large hydrophobic patches in a protein-specific unfavorable local environment. Salt or pH conditions, elevated temperatures, redox stress, or mutations can play important roles leading to unwanted protein-protein interactions and aggregation (24, 26-28).

Until now it is still difficult to measure and interpret aggregation kinetics of different proteins since a deep knowledge of their initial structures, specific transient key intermediates and end-products are necessary (29, 30). The interpretation of folding and misfolding pathways is even more difficult because their respective transient intermediates can be easily mistaken for one another (31). However, in recent years there have been great advances to measure and characterize the structures and aggregation kinetics of especially amyloid fibril forming peptides and proteins (32-35).

1.1.4 Amyloid

Historically, amyloid was discovered as pathological deposits in human diseases, but it is now known that there are also physiological relevant, so called 'functional amyloids', found from bacteria to eukaryotes (36, 37). It has been suggested that almost any protein or polypeptide can aggregate and form amyloid fibrils in solution if incubated under the right conditions (38). Surprisingly, there are only 37 peptides or proteins known to form extra- or intracellular amyloid deposits in human pathologies, raising the questions which intrinsic properties of the polypeptide chain, cellular conditions and mechanisms prevent non-native fibrillar aggregation and toxicity, considering the large size of the human proteome (39, 40). One part of the answer to this is that cells have evolved a large integrated network of molecular chaperones that help to prevent unwanted protein aggregation through different mechanisms.

From a molecular point of view amyloid fibrils are protein homopolymers that form highly ordered double-layered β -sheet structures following the fibril axis, and the β -strands run perpendicularly to the fibril axis (33). As a side note, these features separate amyloid fibrils structurally from for example actin filaments that have mixed secondary structural elements. Amyloid fibrils are characterized by a high affinity for the dye Congo red, resulting in green, yellow or orange birefringence under polarized light, and have distinctive X-ray diffraction patterns (41). The typical amyloid fibrils are unbranched, composed of 2 or more protofilaments, have a diameter of about 70-200 Å and can be several μm long (42, 43). This conformation is highly stable as it most likely resides in an even lower Gibbs free energy minimum compared to the native fold (Figure 2) (44). An overview of the current picture of the free energy landscape of protein folding including amorphous aggregates, amyloid fiber pre-states (oligomers and protofibrils) as well as amyloid fibers are represented in Figure 2. Even though amyloid is known since more than a hundred years it is still a "hot" topic in basic research as there is a lot more to learn about the highly dynamic heterogeneous and polymorphic aggregation mechanism, associated toxicity and effects of aggregation modulators.

1.1.5 Amyloid formation

One of the most studied amyloid fibril forming peptides is the AD-related A β peptide (34, 45). Proteolytic processing of A β PP generates A β peptides of different lengths, of which the 42-residue variant A β ₄₂ is the most aggregation-prone and toxic (46). A β ₄₂ is very "sticky" and has a high tendency to self-associate, ending in the formation of large fibril agglomerates, as seen in senile plaques (47). Even though many proteins and peptides are shown to form

amyloid fibrils in solution, most of them require harsh denaturing conditions, as for example high temperature or a strong acidic environment, under which it is difficult to determine interactions with other proteins (48). It turned out that the A β ₄₂ peptide is an excellent model substrate to study amyloid self-assembly mechanism, since A β ₄₂ fully fibrillates under physiological conditions, in the low micromolar range and on a short time scale (47). This allows to investigate the effects of for example molecular modulators on A β ₄₂ fibril formation and dissect their mechanism of action.

Amyloid fibril formation in general displays sigmoidal growth kinetics, characteristic of a nucleation-dependent polymerization process (Figure 3) (49). The sigmoidal shaped profile can be divided into three phases: a lag phase, a growth phase and a plateau phase. During the lag phase, no fibril formation is detectable but unstructured monomers start to interact with each other and form various sized small metastable assemblies (oligomers), a process referred to as primary nucleation. After reaching a critical oligomer concentration, protofibrils and highly structured β -sheet rich fibrils form. The fibrils can be elongated at the ends and serve also as a reaction surface for the formation of new oligomers in an exponentially accelerated manner, called secondary nucleation. When all monomers are converted into fibrils, the growth ends and the plateau phase is reached (50). This is a very simplistic description of the dynamic heterogeneous self-assembly mechanism and it is important to note that primary nucleation, secondary nucleation, elongation and also fragmentation of fibrils occur during all phases. However, the reaction rates vary together with the concentrations of certain species during the time course of the experiment. The reaction rates and their contributions to the overall aggregation mechanism is highly dependent on the substrate and the experimental conditions. For example, the introduction of shear forces by agitation will increase fragmentation of fibrils, which will increase the number of accessible fibril ends and consequently affect the elongation rate constants. In recent years, reproducible measurements of amyloid fibril formation made it possible to develop mathematical models to describe the macroscopic aggregation profiles by microscopic rate constants and eventually describe the self-aggregation mechanism under numerous conditions and in presence of molecular modulators (32, 47, 51-56). Some insights into the kinetic analysis are given in chapter (3.2.2).

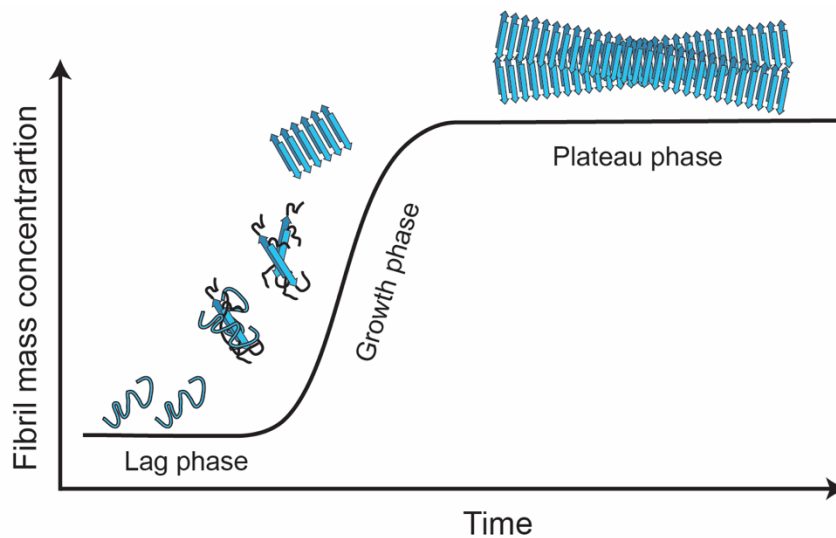


Figure 3: Schematic illustration of the sigmoidal growth kinetics of amyloid fibril formation showing the three phases of fibrillar growth. It is important to note that this is a very simplistic picture of amyloid fibril formation and at each time point a heterogenous mixture of different species is present.

1.2 PROTEIN AGGREGATION DISORDERS

Protein synthesis and folding are complex processes where a plethora of molecular machines are involved, and many things can go wrong. A study using different human cells even suggested that about 30 % of all newly synthesized cellular proteins never make it to their native structure, but get degraded by the proteasome (57). Despite the high capacity to recycle defective produced proteins, cells can get overwhelmed if they are generated at a too high rate. Diseases that are linked to the aggregation and accumulation of misfolded or aggregation-prone proteins are referred to as protein aggregation disorders and can be subdivided into amyloid and non-amyloid disorders (Tables 1 and 2). Amyloid-associated disorders are relatively clearly characterized by an abnormal accumulation of aggregated protein in extra- or intracellular deposits with biochemical characteristics of amyloid. In contrast, non-amyloid-associated disorders are more diverse comprising near-native, amorphous or fibrillar (but non-amyloid) aggregated protein deposits. Nevertheless, it is important to keep in mind that this classification is based on the structural features of the final observable protein deposit but transient intermediate species with different structures occur. During amyloid formation, for example early aggregates show little amyloid features and it has been shown that also in amyloid diseases disordered off-pathway aggregates exist (58). In some cases, classification is still under debate (*e.g.* SOD1) and in others the involved peptide or protein appear in both groups as different types of aggregates are found in different diseases (*e.g.* immunoglobulins).

1.2.1 Amyloid-associated disorders

Intra- or extracellular amyloid deposits in the brain are a common feature in a variety of neurodegenerative disorders, such as AD, and Parkinson's disease (PD) but amyloid deposits are also found in other organs like the lung (interstitial lung disease (ILD)) or pancreas (type II diabetes). To date, there are 37 proteins or peptides identified to form extra- or intracellular amyloid, like the AD related A β peptide or the ABri and ADan peptides derived from mutant Bri2 protein, involved in familial British and Danish dementia (FBD and FDD, respectively) (39, 41, 59). The dementias include a wide range of neurological disorders, like vascular dementia and Creutzfeldt-Jakob disease, which all are characterized by a loss in memory and other cognitive impairments (60). During my studies we were mostly working with the A β peptide and therefore I will briefly introduce AD, but Table 1 contains a selection of peptides and proteins that are found in amyloid-associated disorders.

AD is the most abundant disease among the dementias, accounting for an estimated 60-80 % of all cases. Since age is the greatest risk factor for AD and other dementias, the total number of affected people is predicted to increase dramatically, based on current demographics (61). AD patients show an irreversible decline in cognition, overall functioning and behavior, thereby diverging dramatically from a normal aging process (62). Clinical diagnosis during early stages of AD is still challenging and definitive assessment is only possible by the detection of disease-specific extracellular neuritic amyloid plaques and intracellular tangles in the brain, that contain primarily A β and hyperphosphorylated tau, respectively. These amyloid deposits occur mainly in brain areas correlated with memory functions, like the hippocampus and other medial lobe structures (63, 64).

Table 1: Selection of peptides and proteins found as amyloid in human diseases. The number of residues corresponds to the length of the disease-relevant aggregated form. Adapted from (39) and (65).

Peptide or protein	Number of residues	Associated disease
<i>Neurological disorders</i>		
Amyloid- β peptide (A β)	40 or 42	Alzheimer's disease
α -Synuclein	140	Parkinson's disease
ABri	34	Familial British dementia
ADan	34	Familial Danish dementia

Tau protein	352–441	Frontotemporal dementia with parkinsonism (FTDP)
Huntingtin with polyQ expansion	~3,144	Huntington's disease
Prion protein (PrP)	208	Spongiform encephalopathies (Creutzfeldt-Jakob disease)
Superoxide dismutase 1 (SOD1) [†]	154	Amyotrophic lateral sclerosis (ALS)
<i>Non-neurological disorders</i>		
Lung surfactant protein C (SP-C)	35	Interstitial lung disease
Islet amyloid polypeptide (IAPP)	37	Type II diabetes
Transthyretin (TTR)	127	Senile systemic amyloidosis
Insulin	30 + 21	Injection-localized amyloidosis
Serum amyloid A protein (SAA)	45–104	AA amyloidosis
Proteins S100A8/A9	92/113	Prostate cancer
Fibrinogen	45–81	Fibrinogen amyloidosis
Lysozyme (LYS)	130	Lysozyme amyloidosis
Leukocyte cell-derived chemotaxin-2 (LECT-2)	133	LECT2 amyloidosis

[†] Still under debate if deposits are considered amyloid or non-amyloid.

Even though amyloid fibrils have common structural features and deposits of aggregated peptides and proteins are found in diseases, there is still a lot more to learn about the molecular mechanisms how and to what extent they contribute to each disease. This is aggravated by the fact that the aggregation mechanism in each disease is substrate-specific and that modulators, like molecular chaperones play more important roles. In AD research, for example, a lot is known about the generation of the A β peptide but little about its aggregation mechanism at molecular detail *in vivo* and the correlation with neurodegeneration. From a neuropathological perspective, the extracellular A β plaque burden does not correlate well with cognitive impairment and surprisingly, diffuse amyloid plaques can be found in *postmortem* brain tissues of healthy individuals (66, 67). These observations are interesting from two aspects, first of all the formation of diffuse plaques in a normal aging process could indicate that some individuals are able to modulate the amyloid aggregation

pathway bypassing toxic species, and secondly that these amyloid fibers could structurally differ from the ones found in AD patients. Indeed, some studies show that the levels of soluble low molecular weight A β aggregates, supposedly toxic oligomers, correlate better with cognitive decline (68-72) and structures of AD patient-derived amyloid fibrils show that amyloid fibrils are indeed polymorphic (34, 73). Besides these macromolecular changes, AD and many other aggregation disorders, remain multifactorial diseases where factors like inflammation or oxidative stress play important roles. This leaves many open questions about the mutual dependency of all these factors and, consequently, it remains to be established which screws that are the right ones need to be turned in order to modulate disease.

1.2.2 Non-amyloid-associated disorders

When talking about protein aggregation disorders or misfolding diseases the context is often limited to amyloid-associated diseases. However, from a molecular perspective, mature amyloid fibrils are structurally different from amorphous or native-like aggregates and their aggregation mechanisms and interactions with molecular chaperones are likely very different. In order to emphasize the importance of non-amyloid-associated disorders, some peptides and proteins that are found in human diseases are listed in Table 2.

Table 2: Selection of peptides or proteins deposited as non-amyloid in human diseases. The number of residues corresponds to the length of the disease-relevant aggregated form. Adapted from (39) and (65).

Peptide or protein	Number of residues	Associated disease
<i>Neurological disorders</i>		
Neurogenic locus notch homolog protein 3 (Notch 3) ectodomain	1,589	Cerebral autosomal dominant arteriopathy with subcortical infarcts and leukoencephalopathy (CADASIL)
Actin	375	Alzheimer's disease
Ataxin-1	815	Spinocerebellar ataxia 1
Superoxide dismutase 1 (SOD1) [†]	154	Amyotrophic lateral sclerosis (ALS)

<i>Non-neurological disorders</i>		
γ -Crystallins	variable ~180 (74)	Cataract
Hemoglobin	574 (tetramer)	Sickle cell anemia
Fibronectin (FN)	2,355	FN glomerulopathy
Cystic fibrosis transmembrane conductance regulator (CFTR)	Various fragments	Cystic fibrosis
(75, 76)		

† Still under debate if deposits are considered amyloid or non-amyloid.

1.3 PROTEIN HOMEOSTASIS

The cellular environment is highly crowded where proteins are suggested to reach total concentrations of around 150-300 mg/ml, making correct folding of nascent polypeptides a difficult process (77). Nevertheless, it is important that proteins of a cell fold correctly and remain in a fine-tuned balance also under changes in the intra- and extracellular environment. This condition is referred to as protein homeostasis (proteostasis), which is achieved by controlling the concentration, conformation, binding partners and localization of proteins through the proteostasis network (PN) (78). If the PN is perturbed, newly synthesized proteins might not fold efficiently or adopt non-native conformations in which they can lose their function or even gain toxic activities. Especially, chronic production of aberrant proteins during aging or due to stress conditions can push the PN towards and over its limits and lead to the accumulation of toxic protein aggregates that are associated with multiple diseases (see Tables 1 and 2) (78-80).

1.3.1 Protein quality control

As a safety mechanism, eukaryotic cells possess several protein quality control systems (PQCSs) that govern correct folding of proteins, prevent protein aggregation and remove cytotoxic assemblies. PQC occurs during all stages of a protein's lifecycle from synthesis to degradation and takes place co- and post-translationally (81, 82). Especially, the synthesis of large proteins with several domains is a delicate process where unfolded segments are susceptible to aggregation and therefore need to be protected during translation and folding. One example where cells can regulate the quality of newly synthesized proteins early on is by controlling the mRNA composition and structure, which affects the speed of translation. In turn, the translation rate determines the time during which the nascent chain can fold and molecular chaperones are able to bind exposed aggregation-prone regions, in order to protect

them from unwanted interactions and misfolding (83, 84). However, co-translational protein quality control is regulated in many other ways that involve for example interactions of the ribosome with the polypeptide chain or enzymatic modifications of the nascent chain (82).

After synthesis, folding and assembly, proteins are still exposed to various stresses in their physiological milieu, or by external insults like heat, oxidative stress, toxic substances or mechanical damage. To deal with non-native or aggregated proteins, cells invest in another line of defense, called the post-translational quality control. Central to this defense are numerous molecular chaperones that work together to promote the correct fold of proteins, by targeting incorrectly folded variants. Subsequently, they are capable to “hold”, refold, disaggregate misfolded substrates or participate in proteasomal degradation by the ubiquitin-proteasome system and autophagy (81, 85). Additionally, cells have developed pathways to sequester aggregated proteins in specialized compartments in case the capacities of the PQCSs are exceeded, which helps to protect the cellular environment from harmful consequences of ultimately aggregated and potentially toxic proteins (86, 87).

1.3.2 Molecular chaperones

A molecular chaperone is defined as a protein that stabilizes or promotes folding of another protein, without being part of the final structure (88). The most famous group of molecular chaperones are the heat-shock proteins (HSPs). Their name originates from the finding that the expression of several proteins in fruit flies was upregulated in response to heat stress, which is a straightforward experimental treatment (89). However, also other environmental factors, like oxidative stress, heavy metals or inflammation that increase the concentration of aggregation-prone folding intermediates raise HSP levels. Despite this stress-dependent activation, molecular chaperones also maintain cellular protein homeostasis under normal conditions by promoting folding into native states over aggregation (17, 90). Historically, Laskey and coworkers discovered in 1978 the assembly factor nucleoplasmin that is required for the formation of nucleosomes, an ordered unit of DNA around histones. Nucleoplasmin was shown to interact with histones and prevent their precipitation. This was the first direct evidence for the existence of a molecular chaperone (91). In general, molecular chaperones are involved in many different processes, like preventing aggregation, augmenting folding/unfolding, assisting in assembly processes or enhancing degradation of misfolded proteins. The underlying mechanism of action of each molecular chaperone are highly diverse and not always fully understood. However, there is a common perception that molecular chaperones reduce the probability of unspecific inter- and intramolecular

interactions of their substrates, which they likely recognize by exposed hydrophobic surfaces (17, 22, 90, 92).

Molecular chaperones are roughly divided into two groups based on their ability to bind and consume ATP and the HSPs are further classified according to the molecular weight of their first-identified family member, upregulated under heat-shock conditions. The literature concerning molecular chaperones is extensive and the nomenclature becomes quite confusing if one compares chaperones between different families and organisms. There are the HSP families: HSP40, HSP60, HSP70, HSP90, HSP110 as well as the small HSP (sHSP). Each of these families contain several proteins with similar functions and domains but might have slightly different molecular weights, as indicated by their name, due to for example splice variants. For the human HSP families a new nomenclature has been proposed, based on a classification through conserved structural motifs. The new proposed abbreviation for the human HSPs is indicated in brackets: HSP40 (DNAJ), HSP70 (HSPA), HSP90 (HSPC), HSP110 (HSPH), sHSP (HSPB), and the chaperonin families HSP60/HSP10 (HSPD/E) and TRiC (also known as CCT) (93).

The ATP-dependent chaperones HSP70 (HSPA), HSP90 (HSPC), HSP110 (HSPH) and the chaperonins are multicomponent molecular machines that participate widely in protein folding, unfolding and refolding (17). They are able to recognize exposed non-native structural motives and help proteins, via repetitive cycles of substrate binding and release, to adopt their native conformation or prepare them for degradation. Additional cofactors and co-chaperones, like sHSPs (HSPB) and HSP40 (DNAJ) enhance their binding efficiency and specificity (17, 94). ATP-independent molecular chaperones on the other hand block protein aggregation in an energy-independent manner. Since the BRICHOS domain possesses characteristics, similar to ATP-independent molecular chaperones, the next paragraph is dedicated to describing this group of proteins in more detail.

1.3.3 ATP-independent molecular chaperones

ATP-independent molecular chaperones are able to maintain substrates in a folding competent state without refolding them and therefore are often referred to as “holdases”. By keeping their clients in near-native conformations, they allow efficient refolding or degradation by downstream ATP-dependent molecular chaperones (95). ATP-independent molecular chaperones respond to a myriad of stresses and are extremely diverse in their structures and modes of action. Some members have additional chaperone-independent functions and their molecular chaperone functions become more dominant under stress

conditions. Examples are thioredoxin (Trx) as reductase (96), α 2-Macroglobulin as broad-spectrum protease inhibitor in human blood (97) or Get3 which is involved in the integration of tail-anchored (TA) proteins in the membrane of the endoplasmic reticulum in yeast (98). But are there some common structural characteristics and activation mechanisms that are shared by ATP-independent molecular chaperones? There is no universal answer to this question but one feature that many ATP-independent molecular chaperones have in common is that they possess a high degree of conformational flexibility and are able to transit between low- and high-affinity states for non-native client proteins (99). Some ATP-independent molecular chaperones, for example, form polydisperse high molecular weight (HMW) assemblies where either oligomerization from smaller subunits (*e.g.* Get3 (98)) or dissociation of the oligomers into smaller species (*e.g.* α B-Crystallin (100)) is important for their activation. But also increasing substrate affinity through structural changes in the oligomer substructure (*e.g.* α -Crystallin (101)), or partial unfolding of the monomer conformation in order to dimerize (*e.g.* Hsp33 (102)), as well as simple overexpression of an active chaperone (*e.g.* Spy (103)) have been demonstrated. The dynamic behavior in most cases of ATP-independent molecular chaperones is key to their function, as it enables them to adequately respond to stress insults by shifting the equilibrium towards the most active conformation.

Conditions that regulate ATP-independent molecular chaperone plasticity and activity are as diverse as this protein family itself. It has been shown that (1) the presence of unfolded or partially folded clients (104); (2) changes in the environmental conditions (pH, temperature, redox,...) (102, 105, 106); (3) post-translational modifications (100) and, (4) the formation of heteroassemblies between different molecular chaperones (107) modulate their activity. This broad spectrum of structural and functional triggers likely reflects the stress-specific response for each ATP-independent molecular chaperone. However, this does not necessarily mean that there is only one molecular chaperone responding to one unique stress condition. Furthermore, it is very likely that ATP-independent molecular chaperones have distinct but also overlapping substrate spectra (108).

Another fascinating question that comes up when one thinks about ATP-independent molecular chaperones is the reason for their existence, considering that ATP-dependent molecular chaperones that are able to refold or degrade substrates are highly abundant in organisms. Two reasonable arguments are that ATP-depletion under stress conditions and low-level ATP compartments, like the extracellular space were the driving force for their evolution. Under these conditions, ATP-independent molecular chaperones are rapidly

activated and comprise a functional reservoir of proteins that can protect the proteome from harm (109). However, these explanations do not sufficiently reason the existence of ATP-independent molecular chaperones in ATP rich compartments, like the cytosol or mitochondria, even under non-stress conditions. It was suggested that the structural diversity and mode of substrate recruitment are different for ATP-independent molecular chaperones compared to ATP-dependent molecular chaperones and consequently expand the substrate spectrum, as well as binding and refolding efficiency of ATP-dependent molecular chaperones (109). Nevertheless, there might be additional, yet unknown reasons for their evolution.

Taken together the plasticity of ATP-independent molecular chaperones substantially contribute to the basal cellular homeostasis, protects the proteome during stress conditions and likely plays an important protective role in a number of human diseases that are characterized by the accumulation of aggregated proteins, like AD, PD and cataract.

1.4 THE BRICHOS PROTEINS

In 2002 Sánchez-Pulido and colleagues described a novel protein sequence motif found in several unrelated proteins that are linked to a variety of diseases, like dementia, respiratory distress and cancer. The so-called BRICHOS domain, named after the protein family members BRI2, CHONDromodulin-I and proSURfactant protein C (proSP-C) are found in 10 human protein families of which two, namely Bri2 and proSP-C, are associated with amyloid formation (110, 111). The BRI family has members in ancient species like flies and worms and might be the oldest family of proteins that contain a BRICHOS domain (110). Later, Hedlund and coworkers refined the characterization of the BRICHOS proteins by integrating amino acid side chain properties and secondary structure predictions. They discovered that generally all BRICHOS domains span about 100 amino acid residues and likely possess a unique fold. The BRICHOS domains from different families have low pairwise sequence identities (down to ~20 %) but a strong consensus in their predicted secondary structures, suggesting that the BRICHOS structure is widely preserved. Thus, it was hypothesized that all BRICHOS domains share some functional properties but may have evolved different specific functions. It is interesting to note that there are just three amino acids that are strictly conserved, one aspartic acid (Asp) and two cysteine (Cys) residues. The regions around the Cys have the highest sequence similarities (112). Until now only the structure of proSP-C BRICHOS has been solved showing that the two conserved Cys form an intramolecular disulfide bond, and their strict conservation suggests that this disulfide bridge is present in all BRICHOS domains (111, 113).

BRICHOS containing proproteins are known or predicted to be type II transmembrane (TM) and secretory proteins that share a similar architecture of a N-terminal cytosolic domain, a hydrophobic TM region or signal peptide, a linker region, a BRICHOS domain and a C-terminal domain that has a high propensity to form β -sheet rich structures (Figure 4A). The only exception is proSP-C that lacks the C-terminal domain but has an aggregation-prone TM region (Figure 4B) (110, 112). Since my studies mainly focus on the BRICHOS domains from proSP-C and Bri2, I will review them and their precursor proteins in more detail.

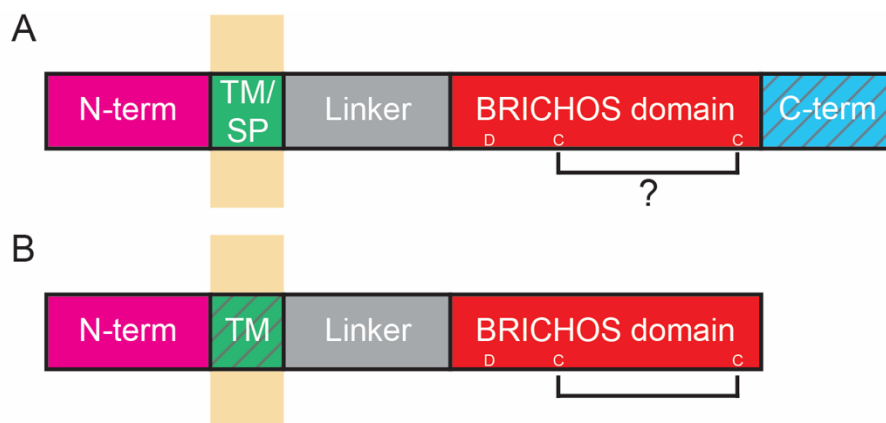


Figure 4: Schematic overview of the general BRICHOS protein architecture of (A) all BRICHOS domain containing proteins except proSP-C, which is shown in (B). The N-terminal domain is highlighted in magenta, the TM region or signal peptide (SP) in green, the linker in grey, the BRICHOS domain in red, the C-terminal region in blue and the membrane segment in yellow. The strictly conserved Asp (D) and Cys (C) residues are labeled and the intramolecular disulfide bond of the two Cys is indicated. The aggregation-prone regions are shown with grey stripes.

1.4.1 Prosurfactant protein-C (proSP-C)

Lung surfactant proteins maintain the stability and spreading of the surfactant phospholipid layer in the alveoli. It covers the inside of our lungs in order to prevent them from collapsing at the end of expiration and protect them against microbial pathogens. Therefore, these proteins are important and malfunctions (caused by mutations or lung injuries) are associated with severe respiratory dysfunction (114).

Surfactant protein C (SP-C) is a 35 amino acid protein, which is exclusively produced in alveolar type II epithelial cells, via proteolytic processing of the 197 residues spanning precursor protein proSP-C (115, 116). ProSP-C is synthesized in the endoplasmic reticulum (ER) where it is inserted into the ER membrane in a type II orientation (the N-terminus is facing the cytosol and the C-terminus the lumen of the ER). The TM region makes up major parts of SP-C (116, 117). Along the secretory pathway proSP-C becomes 1) palmitoylated in the N-terminal region of the TM/SP-C part, 2) transferred into multivesicular bodies, 3)

processed in a multistep fashion, first at the C-terminal end, followed by the N-terminal part and 4) packed into lamellar bodies for secretion into the air space together with phospholipids (118-120).

Mature SP-C mainly adopts an α -helical conformation in the lipid bilayer and it is one of the most hydrophobic proteins known with more than 80 % non-polar residues and its central hydrophobic domain is comprised of an isoleucine and valine rich region (121, 122). Both these amino acids are known to be abundant in β -sheet rich structures and are predicted to have a high propensity to form amyloid (123, 124). Mutations in the proSP-C gene (*SFTPC*) are associated with ILD that is characterized by intracellular protein aggregates (125, 126). Interestingly, most disease-causing mutations are located in the linker region or in the BRICHOS domain leading to abnormal processing and trafficking (127). Abnormal processing was also observed by expressing C-terminally truncated mature proSP-C constructs in a lung epithelial cell line, suggesting an important function of the BRICHOS domain (128). Furthermore, expression of mature SP-C in transgenic mice leads to severe pathology (129). Therefore, it has been suggested that the BRICHOS domain works as an intramolecular chaperone domain, guiding the aggregation-prone TM region into the correct conformation and preventing β -sheet aggregation (111).

1.4.2 Integral membrane protein 2B (ITM2B) - Bri2

The Bri2 protein is a type II TM protein encoded by the integral transmembrane protein 2B (*ITM2B*) gene, which is expressed in high levels in the brain and many peripheral tissues, like the placenta, kidney or pancreas (130). Full-length Bri2 comprises 266 amino acids, consists of an N-terminal cytosolic part (residues 1-54), a TM region (residues 55-75), a linker (residues ~76-130), a BRICHOS domain (residues ~130-231) and a C-terminal region (residues 232-266) (131) and undergoes several proteolytic processing steps within the secretory pathway (Figure 5). At first Bri2 is cleaved in the C-terminal region, which releases a 23 residues peptide (Bri23) and a membrane-bound N-terminal part called mature Bri2 (mBri2) (132, 133). The cleavage is most likely not exclusively performed by a single protease but data indicate furin as the main protease (132). Nevertheless, several other proprotein convertases have been shown to process Bri2, although less efficiently than furin (134). The membrane-associated mBri2 is further shed by the α -secretase ADAM10, cleaving in the linker region close to the suggested BRICHOS domain, which is subsequently released into the extracellular space (135). The exact position of the cleavage site is still unknown but for A β PP it has been shown that ADAM10 cleavage is not primary structure-specific but rather depends on the distance from the plasma membrane (136). Processing by ADAM10

leaves a membrane-bound N-terminal fragment (NTF) of Bri2, which undergoes intramembrane processing by the signal peptide peptidase-like proteases 2a and 2b (SPPL2a/b). As a result, a Bri2 intracellular domain (ICD) as well as a C-domain, which refers to the C-terminal part of the NTF, is released (135).

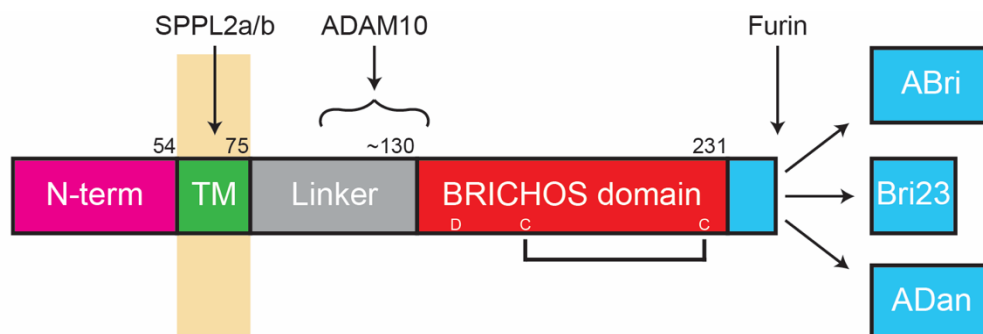


Figure 5: Schematic overview of the Bri2 protein and its processing into fragments. The N-terminal domain is shown in magenta, the TM region in green, the linker in grey, the BRICHOS domain in red, and the C-terminal region in blue. The strictly conserved Cys residues form an intramolecular disulfide in Bri2 BRICHOS monomers (paper I). Numbers indicate the last residue of each region, and the arrows the cleavage sites.

Interestingly, two different autosomal dominant mutations in the *ITM2B* gene lead to the release of extended C-terminal peptides, ABri and ADan, of 34 residues length, that deposit primarily in the CNS as amyloid. These peptides have been found to cause FBD and FDD that share clinical and pathological similarities with AD, in particular amyloid angiopathy and neurofibrillary tangles in the hippocampus (130, 137, 138). There have been two hypotheses suggested for the cause of FBD and FDD. One is that the C-terminal extended peptides aggregate and gain toxic functions similar to A β . The second hypothesis is that mutations in the *ITM2B* gene contribute to a loss of function of the Bri2 protein and redirect it for degradation. The latter theory is supported by data showing that Bri2 modulates the processing of A β PP, implying that decreased levels of Bri2 give rise to increased levels of secreted A β , which in turn lead to disease (139), and by the finding that Bri2 BRICHOS prevents A β fibril formation and neurotoxicity (see further below). There is data supporting both theories and therefore a “two-hit” mechanism where both hypotheses have been integrated has been postulated. Whether one or the other hypothesis or both are true remains to be seen.

1.4.3 Other BRICHOS proteins

The by far most studied BRICHOS proteins are proSP-C and Bri2. However, there are several other less well described BRICHOS families. There are 2 more members in the Bri

subfamily, namely Bri1 and Bri3. Bri1 is predominantly expressed in osteogenic and chondrogenic tissues (140). One *in vitro* study suggests that Bri1 is involved in the early stages of chondrogenesis (141) and another one that Bri1 is important in cell differentiation during odontogenesis (142). Bri3 is mainly expressed in the brain and processed by furin, releasing a C-terminal peptide fragment, which is similar to Bri2. However, compared to Bri2, no shedding and release of the Bri3 BRICHOS ectodomain and intramembrane proteolysis have been observed (143, 144). Both Bri2 and Bri3 are able to modulate processing of A β PP, leading to a reduction of secreted A β peptides (145).

Another subfamily that contains a BRICHOS domain are the gastrokines: GKN1, GKN2 and GKN3. GKN1 and GKN2 are expressed in the gastric mucosa in humans. They are associated with gastric cancer and their expression is downregulated in gastric adenocarcinoma tissues (146, 147). Even though GKN1 is a stomach-specific protein it has also been reported to inhibit A β ₄₀ fibril formation and interact with endogenous A β PP in a GKN1 transfected neuroblastoma cell line. It was suggested that these attributes are correlated to the BRICHOS domain in GKN1 (148). In contrast to GKN1 and GKN2 the GKN3 gene has a premature stop codon in humans but is functional in other mammals, including mice. In mice, GKN3 is upregulated in gastric atrophy and might limit epithelial cell proliferation under this condition (149).

Chondromodulin-1 (CHM-1, alternative name: leukocyte cell-derived chemotaxin 1) is most abundantly expressed in cartilage and cardiac valves and is important for promoting chondrocyte differentiation and inhibition of angiogenesis. Decreased levels of CHM-1 are found in association with chondrosarcoma (150, 151). Tenomodulin is most abundant in dense connective tissues and skeletal muscle, and its expression correlates well with the embryonal differentiation of tendon fibroblasts in chick (152, 153). BRICHOS proteins of the group C family have only been studied on the gene level and according to their sequence and secondary structure conservation. It is interesting that the group C family has the highest conservation in the C-terminal region among all BRICHOS families, indicating an important function of this region (112). Proteins of the Arenicin family are so far only found in marine worms. They differ from other BRICHOS families as the transmembrane region contains a signal peptide and the C-terminal region has been shown to be an anti-microbial peptide (154).

1.5 THE BRICHOS DOMAIN

1.5.1 Structure

So far, the only available high-resolution structure of a BRICHOS domain is the crystal structure of recombinant human (rh) proSP-C BRICHOS (Figure 6A). The core consists of a mixed anti-parallel and parallel five-stranded β -sheet that is flanked by two α -helices. Helix 1 packs against face A, helix 2 against face B and a long loop connects both helices (111). Homology models of all human BRICHOS families based on the X-ray structure of proSP-C BRICHOS largely match their predicted secondary structures, especially in the core region, illustrated for Bri2 BRICHOS (Figure 6B) (155). As mentioned earlier there are just three residues that are highly conserved among all BRICHOS proteins, two Cys and one Asp (112). These two Cys in proSP-C BRICHOS and Bri2 BRICHOS form an intramolecular disulfide bond that links helix 2 and face B in proSP-C BRICHOS, and likely also in Bri2 BRICHOS (111). This disulfide bond might increase the stability of the BRICHOS domains and could play an important role in the regulation of their function. Human proSP-C BRICHOS has two additional Cys that form another intramolecular disulfide bond between the loop region just after helix 1 and face A, which likely has an impact on the dynamical properties of the domain, although it is not conserved among the proSP-C BRICHOS family. Molecular dynamic (MD) simulations of the proSP-C BRICHOS structure revealed that movement of helix 1 exposes face A, which is supposedly the binding site for substrates (111). This fits very well with the observation that face A has mostly hydrophobic amino acids that match the hydrophobic SP-C target sequence. In contrast Bri2 BRICHOS has several charged sidechains in face A, which goes in line with the properties of the proposed target sequence of Bri23. This suggests a correlation between the proposed binding sites of the BRICHOS proteins and their target peptides (155). Furthermore, many conserved residues in the proSP-C family are located in the β -sheet face A and B, and mutations seen in ILD largely coincide with the strictly conserved amino acids (111). *In vitro*, rh proSP-C BRICHOS forms stable trimers that are stabilized by non-covalent interactions and a salt bridge between the subunits (Figure 6C). Peptide binding experiments using mass spectrometry (with collision-induced dissociation) show that monomers bind designed model peptides with apparent dissociation constants in the micromolar range (156). Furthermore, addition of detergents that increase the monomer/trimer ratio also improve the efficiency to inhibit A β ₄₂ fibril formation, supporting the theory of the monomer being the active species and the trimer the storage conformation (157). The role of the strictly conserved Asp has not been elucidated to date, albeit MD simulations comparing wild-type (WT) and an Asp to Asn (asparagine) substituted variant show that the face A in the WT, but not in the Asp to Asn

variant becomes accessible for substrates at moderately elevated temperatures. This suggests that the Asp contributes in some way to the dynamics of proSP-C BRICHOS and may regulate its binding properties (111).

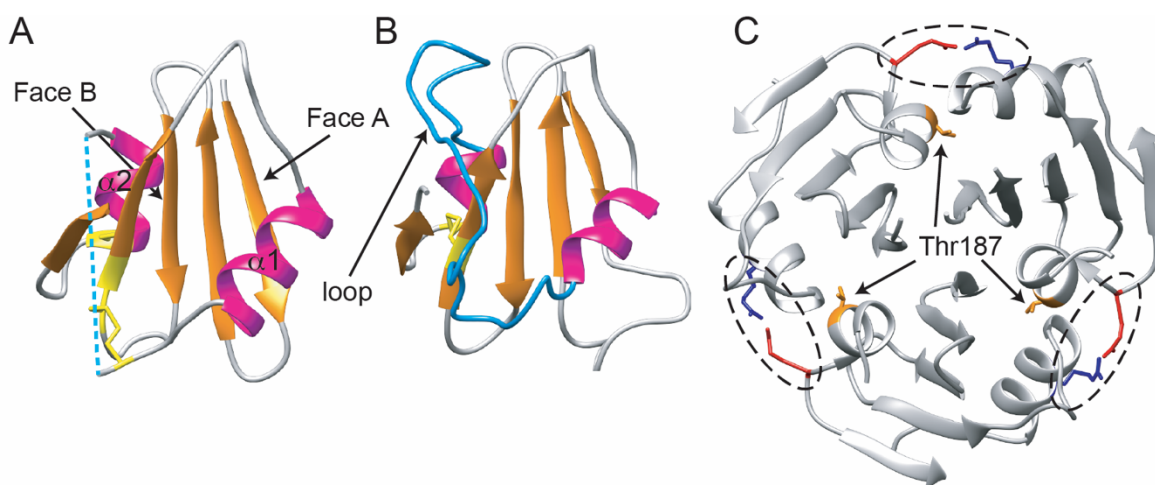


Figure 6: (A) Crystal structure of the proSP-C BRICHOS domain (PDB ID: 2yad). Both sides of the central five-stranded β -sheet are labeled, the intramolecular disulfide bonds are shown in stick representations (yellow) and the loop (which is missing due to proteolytic cleavage) that connects both α -helices ($\alpha 1$ and $\alpha 2$) is indicated with a dashed line. (B) Structural model of the Bri2 BRICHOS domain (I-Tasser web server (158)) with the same color coding as in A. (C) Crystal structure of the proSP-C BRICHOS domain in the trimer conformation (PDB ID: 2yad). The salt bridges that stabilize the trimer are highlighted with dashed ellipses and the threonine residues at position 187 (T187) that are located in the interface between each subunit of the trimer are shown in orange stick representations (see 4.1).

1.5.2 Function

It has been shown that rh proSP-C BRICHOS and Bri2 BRICHOS efficiently delay $A\beta_{40}$ and $A\beta_{42}$ fibril formation *in vitro* and improve the longevity and locomotor activity in an $A\beta_{42}$ overexpressing fly model (159-164). However, the two rh BRICHOS domains show different effects on the kinetics of $A\beta_{42}$ fibrillation. While proSP-C BRICHOS binds to fibril surfaces and blocks secondary nucleation events, Bri2 BRICHOS additionally inhibits the elongation of already formed fibrils (160). Furthermore, it has been shown that both rh BRICHOS domains reduce neuronal network toxicity evoked by $A\beta_{42}$ in hippocampal mouse brain slices (53, 161, 165). Interestingly, only rh Bri2 BRICHOS is able to prevent non-fibrillar aggregation of different model substrates by forming transient complexes. Poska and co-workers pointed out that Bri2 BRICHOS has no refolding activities and releases no active substrate molecules, but its behavior is appealingly similar to the ATP-independent molecular chaperones sHSP26 and sHSP42 from baker's yeast (161). These sHSP bind non-selectively to misfolded substrates, and thereby prevent them from aggregation. In all experiments it

appears that the Bri2 BRICHOS domain is a more versatile and efficient chaperone than proSP-C BRICHOS.

2 AIMS OF THE THESIS

The studies outlined above describe the proSP-C and Bri2 BRICHOS domains as efficient molecular chaperones to reduce amyloid fibrillation and associated toxicity. In contrast to proSP-C BRICHOS, Bri2 BRICHOS has additional chaperone functions to prevent non-fibrillar protein aggregation, similar to sHSPs. The underlying structural correlations of their distinct functions were, however, largely unknown.

The main aim of this thesis was to investigate and modulate the structure-function relationship of the molecular chaperone domain BRICHOS concerning its ability to prevent structurally different substrates from aggregation.

More specifically:

- ⇒ Study the ability of the Bri2 BRICHOS domain to interfere in the aggregation pathway of structurally distinct substrates in detail (**Paper I**).
- ⇒ Use the information from Paper I and design a Bri2 BRICHOS monomer mutant with increased abilities to prevent amyloid fibrillation associated toxicity (**Paper II**).
- ⇒ Investigate the molecular mechanisms that convert Bri2 BRICHOS monomers, that are essentially inactive in preventing non-fibrillar protein aggregation into active oligomers (**Paper III**).
- ⇒ Expand the BRICHOS repertoire by a functional characterisation of the Bri3 BRICHOS domain that shares about 60 % sequence conservation to Bri2 BRICHOS (**Paper IV**).
- ⇒ Use the knowledge from Paper II and create a proSP-C BRICHOS monomer mutant with the aim to understand the binding spectrum towards small oligomeric species during amyloid fibrillation (**Paper V**).

3 METHODOLOGY

3.1 CHARACTERISATION OF PROTEINS

3.1.1 Circular dichroism spectroscopy

Circular dichroism (CD) spectroscopy is an established method for the determination of the overall secondary structure of proteins (166). CD spectrometers are measuring the absorption difference between right- and left-handed circular polarized light after the light passes through a medium. The amide groups of a polypeptide chain absorb light in the far-UV range (< 260 nm). Furthermore, all naturally occurring amino acids are in the L-configuration which makes proteins chiral. Based on these two physical properties of proteins, the absorption of right- and left-handed circular polarized light is uneven and makes the transmitted light elliptic (circular dichroism). Secondary structure elements in proteins produce characteristic absorption patterns in the far-UV range, that can be related to empirical reference spectra. Especially, helical proteins have a strong CD absorption signal with a characteristic amplitude minimum at 222 nm, but also other secondary structure elements have characteristic signals. Additionally, the side chains of amino acid residues in the protein core have a characteristic CD absorption in the near-UV region (320 – 260 nm) and can give some insights about the tertiary structure of a protein. CD spectroscopy is very useful to study the thermodynamic stability of proteins and mutants thereof by measuring their unfolding behavior for example by increasing the temperature or by adding chaotropic agents (166). CD spectroscopy can also be used to measure the kinetics of amyloid fibril formation, as the transition from monomers with a random-coil like structure to fibrils is correlated with a strong increase in overall β -sheet content (50). Nevertheless, it is important to keep in mind that proteins with mixed secondary structures will result in a CD spectrum where all elements are superimposed. There are plenty of programs that calculate the secondary structure content from CD spectra, but the deconvolution varies a lot dependent on the method. Furthermore, large changes in the conformation of a protein can also result in no observable changes in the CD spectrum, if for example the changes only involve movement of entities with no secondary structure changes or if a high helical content (which has the strongest CD signal) shields other transformations in the CD spectrum.

3.1.2 Mass spectrometry

Mass spectrometry (MS) is a valuable method that can be used to analyze intact proteins and peptides and to detect them qualitatively and quantitatively in complex mixtures. In reference (167) principles of mass spectrometry are well explained. There are numerous of different

set-ups and mass spectrometer configurations that were designed to answer specific research questions. The BRICHOS proteins we investigated are able to form different assembly states and we introduced mutations with the aim to increase the monomer content in the respective BRICHOS domain preparations. For this purpose, we mainly used electrospray ionization mass spectrometry (ESI-MS) first of all to verify the correct masses of our protein preparations and secondly to investigate their quaternary structure.

ESI is a soft ionization method where droplets of a protein solution are dispersed by electrospray and ionized while the solvent around the protein evaporates. This leaves charged molecules in the gas phase that are transferred into the vacuum chamber of the mass spectrometer for analysis. The number of charges on the protein molecules is dependent on the size of the protein and the number of accessible basic residues. In MS, molecules are analyzed according to their mass-to-charge ratio of the ions and a typical spectrum shows the mass-to-charge ratio vs. the ion signal. Short peptides have likely only a few protonation sites and the spectra are relatively simple. Intact proteins on the other hand with multiple protonation sites result in more complex spectra. A pure protein preparation will show a distribution of characteristic clusters containing multiply charged ions. In order to avoid overlapping spectra and a good signal-to-noise ratio it is important to have highly pure samples (salt, for example, will result in strong background noise).

We also used a proteomics mass spectrometry workflow to investigate inter- and intramolecular disulfide bonds in the Bri2 BRICHOS domain. For proteomics analysis, complex protein mixtures are proteolytically digested and in order to reduce the complexity of the sample during mass spectra recordings, the digested peptides are pre-fractionated for example by high-performance liquid chromatography. The peptides are subsequently analyzed by tandem mass spectrometry (MS/MS). First, the peptides are separated according to their mass-to-charge ratio (MS1). Then a particular m/z ratio from the MS1 scans is selected for fragmentation, for example by electron-capture dissociation (ECD) or collision-induced dissociation (CID) and these peptide fragments are then analyzed according to their m/z ratio (MS2). The fragmented peptide spectra from MS2 scans contain information about the peptide amino acid sequence and together with the information from the MS1 scan it is possible to match the sequenced peptide with a protein. This allows the identification of many individual proteins in solution. However, we used this workflow in order to investigate if different Bri2 BRICHOS assemblies form homo- or heterodisulfide bonds under non-reducing conditions in pure protein preparations. For the analysis we created a library containing the theoretical m/z ratios of the proteolytically digested Bri2 BRICHOS domain

(MS1) and a second library with theoretical reference spectra of the fragmented peptides (MS2). Practically we were looking for precursor ions that match the expected m/z ratio of oxidized Cys peptides and match the corresponding MS2 scan against our library.

Even though mass spectrometry is a powerful tool for answering a variety of protein related research questions it has also some limitations. One is that in mass spectrometry one can only find something that one is “correctly” looking for. This means for example, that a protein with an unknown post-translational modification will have a different m/z ratio compared to the non-modified counterpart. However, the experimenter only recognizes a certain mass and does not know if this mass corresponds to a different protein or is due to a modification of a protein. Therefore, it is up to the experimenter to have a good guess in order to match his assumption and interpret the data. Furthermore, the absence of detection in mass spectrometry of a peptide fragment or a protein does not necessarily mean that it is not present in the sample. It could be that this particular peptide fragment is just not being ionized well or that the abundance is extremely low and hence invisible in background noise.

3.2 EVALUATION OF PROTEIN-PROTEIN INTERACTIONS

3.2.1 Fluorescence basics

Absorption is defined as the interaction between a molecule and light whereby the energy of a photon is transferred. Electrons in a molecule can occupy different energy states, dependent on their configuration. The absorption of a photon by a molecule causes an electron transition to a higher electronic and vibrational state. The absorbed energy can be emitted via non-radiative processes such as heat to the solvent or emission of light, termed luminescence. There are two types of luminescence, fluorescence and phosphorescence. Fluorescence involves an electron transition from an excited singlet state to the ground state. On the other hand, phosphorescence is associated with an additional spin conversion (intersystem crossing) and the transition from an excited triplet state to the ground state. Since a molecule cannot emit more energy than it has taken up via the accepted photon and some energy from the excited state always gets “lost” by non-radiative processes, a fluorescent molecule emits light with lower energy. Consequently, the fluorescence spectrum of a molecule is characterized by a red shift in respect to its absorbance spectrum. Molecules that emit fluorescence are called fluorophores (168).

In proteins the amino acids tryptophan, tyrosine and phenylalanine are natural fluorophores and can be used in several fluorescence spectroscopy applications. However, most peptides or proteins have either none of these natural fluorophores or have them in an unfavorable

structural orientation or position. Furthermore, the quantum yield of these three amino acids is not very high compared to other organic fluorophores which might limit their application. To overcome this, numerous fluorescent dyes have been developed with improved quantum yield, photostability and chemical modifications that interact with, stain and label biomolecules.

Two examples of extrinsic fluorophores that we have been using are 4,4'-bis-1-anilino-naphthalene-8-sulfonate (bis-ANS) and Thioflavin T (ThT). Bis-ANS fluorescence depends on the polarity, viscosity and temperature of the environment. Interactions of bis-ANS with a hydrophobic surface lead to an increase of the fluorescence emission intensity and blue shift of the emission maximum (169). Many ATP-independent molecular chaperones expose hydrophobic surfaces in order to interact with their clients. Thus, bis-ANS fluorescence has been used to determine if certain stress conditions lead to an increase in surface hydrophobicity. From these results one cannot conclude if the molecular chaperone is active or inactive, but it can be a piece in the puzzle characterizing a molecular chaperone.

ThT is intensively used to stain amyloid fibrils *in vitro* and to measure the growth kinetics of amyloid fibril formation. This dye is a benzothiazole that has an absorption maximum at ~412 nm in water and exhibits little or no fluorescence. When ThT binds to amyloid fibrils its absorbance maximum shifts to ~440 nm in combination with a strong increase of the fluorescence quantum yield with an emission maximum at ~485 nm. The current knowledge suggests that ThT behaves like a “molecular rotor”. In free ThT a benzylamine and benzothiazol ring can rotate freely around their shared carbon bond and the excited state is rapidly quenched. Once ThT binds to a substrate where rotational quenching is restricted, relaxation of the excited state to the ground state is more likely to occur via fluorescence (169, 170).

3.2.2 Kinetics of amyloid fibril formation

In our studies we exclusively used A β ₄₂ as a model substrate to investigate the effects of different BRICHOS domains to interfere with amyloid aggregation. This chapter is not meant as a detailed manual for the fitting routines and interpretation of the kinetic models that describe the rate constants of A β ₄₂ fibrillation, but rather tries to give a general overview. Detailed descriptions of different kinetic models regarding amyloid fibrillation can be found in references (50, 52, 54).

An important problem in analyzing individual $A\beta_{42}$ aggregation traces is that they *per se* do not contain much mechanistic information. Therefore, global fitting approaches have been developed in order to fit amyloid aggregation data from several varying $A\beta_{42}$ concentrations simultaneously. One important assumption that has to be made and verified before different advanced models can be applied is that the $A\beta_{42}$ monomer concentration at the end point of the reaction (plateau) is neglectable, meaning that almost all monomers have converted into fibrillar mass. One has to keep in mind that once fibrils are formed the kinetic analysis does not account for the dissociation of $A\beta_{42}$ monomers from fibril ends, as this process is relatively slow compared to fibril formation and therefore does not significantly affect the kinetics of fibrillar growth. Additionally, the fluorescence of the reporter dye (ThT) has to scale proportional to the fibrillar mass starting from different initial $A\beta_{42}$ monomer peptide concentrations. With these assumptions in mind and reproducible, high-quality data at hand one can start to evaluate different kinetic models.

In chapter 1.1.5 the general aggregation behavior of amyloid fibril formation and associated nucleation reactions are outlined. In the first step of the analysis the data is normalized to values between 0 and 1, based on the assumption that the relative fibrillar mass across all measured $A\beta_{42}$ concentrations is equal at the endpoint of the experiment and consequently the information on the reaction kinetics are encoded in the shape of curves (52). $A\beta_{42}$ aggregation profiles usually follow a sigmoidal growth behavior (Figure 3) and can be fitted to:

$$F = F_0 + A/(1 + \exp(r_{max}(\tau_{1/2} - t))) \quad (1)$$

where F_0 is the baseline value, A the amplitude, r_{max} the maximum growth rate, and $\tau_{1/2}$ the aggregation half time.

The half time from different kinetic traces is dependent on the initial monomer peptide concentration $m(0)$ and can be expressed through a power law function:

$$\tau_{1/2} \propto m(0)^\gamma \quad (2)$$

where γ is the scaling exponent, $\tau_{1/2}$ the aggregation half time and $m(0)$ the monomer peptide concentration.

The scaling exponent which is the slope represented by $\tau_{1/2}$ vs. $m(0)$ in a double logarithmic plot gives an indication of the reaction order of the aggregation process and suggests if the reaction is truly dependent on the initial $A\beta_{42}$ monomer peptide concentration. Amyloid aggregation can be described by different microscopic mechanisms (*i.e.* primary nucleation,

secondary nucleation, elongation and fragmentation) of which each can have a highly differing impact on the overall aggregation, dependent on the conditions and type of peptide. For example, A β ₄₂ aggregation kinetics with agitation will result in fibril fragmentation, increase the number of fibril ends and therefore increase the impact of elongation on the overall reaction. We used quiescent conditions throughout and it has been shown that monomer dependent secondary nucleation is the dominant process for the formation of new A β ₄₂ aggregates, once a critical fibrillar mass has formed under these conditions (52).

Next, global fit analysis can be performed using aggregation traces with different initial monomer concentrations. The detailed equations are shown in the method sections of paper I, II, IV and V. The global fit expression contains parameters that describe the microscopic rate constants for primary nucleation (k_n), fibril elongation (k_+), and secondary nucleation (k_2) as well as the reaction orders for primary (n_c) and secondary nucleation (n_2). In order to avoid overfitting, the degrees of freedom are restricted and the combined rate constants $\sqrt{k_n k_+}$ and $\sqrt{k_+ k_2}$ are chosen as the only free parameters during the global fitting routine. For extracting individual rate constants another set of experiments with a high initial concentration of fibrillar seeds is needed. In this experiment, the aggregation traces normally exhibit a concave profile, where the initial slope is directly proportional to the fibril elongation rate (k_+). This can be explained by the high number of fibrils that are already present at $t=0$ h and elongation is dominating over primary and secondary nucleation. This fitting procedure enables us to describe the microscopic rate constants of amyloid fibril formation and can be applied to investigate the effects of different aggregation modulators on individual rate constants. One important note that I would like to add is that an inhibitory effect on secondary nucleation reactions is sometimes directly linked to the notion of a decreased number of toxic oligomers and therefore an amyloid modulator might be an important drug candidate. However, toxic A β ₄₂ oligomers are not part of the fitting analysis but rather concluded from an inhibitory effect on the secondary nucleation rate constant. Indeed, several studies have shown that if an inhibitor shows strong effects on the rate constants for secondary nucleation, additional toxicity experiments seem to confirm the assumption (53, 171, 172). Nevertheless, there is another study demonstrating that an aminosterol enhances the overall rate of A β ₄₂ aggregation by increasing secondary nucleation reactions but still decreasing A β ₄₂-induced toxicity (173). This is counterintuitive, but the authors concluded that enhancing secondary nucleation will also speed up the conversion of oligomers to mature fibrils and hence bypass toxic species more rapidly. In summary, it remains to be seen what the best way is to reduce

neurotoxicity in human amyloid associated diseases, but it seems that modulating secondary nucleation pathways is a promising approach.

3.2.3 Fluorescence correlation spectroscopy

Fluorescence correlation spectroscopy (FCS) is a powerful tool to investigate the molecular properties of a fluorescent molecule in solution or to determine interactions and binding constants between molecules. A typical FCS set-up consist of a confocal fluorescence microscope with a small detection volume, avalanche photodiode detectors to detect the emitted photons and a hardware correlator that can calculate the autocorrelation function $G(\tau)$. The following description is based on references (174, 175).

In FCS stochastic fluctuations arising from Brownian motion of fluorescent molecules in a small observation volume element (OVE) are measured over time and the recorded fluorescence signal is analyzed using autocorrelation (Figure 7). The autocorrelation analysis determines the relationship between two observations of fluctuating molecules in a time series and determines a pattern in this series. From this, the autocorrelation function describes characteristic time constants and amplitudes for molecules in the OVE. Any molecular event that causes fluctuations in the fluorescence intensity results in a characteristic decay of the $G(\tau)$, which is calculated from the time-trace of the fluorescence intensity $I(t)$. $G(\tau)$ is described by:

$$G(\tau) = \frac{\langle I(t) + I(t + \tau) \rangle}{\langle I(t) \rangle^2} \quad (3)$$

Figure 7A shows the movement of a fluorescent molecule in a confocal volume that is being detected and analyzed by FCS. Diffusion of the particles cause changes in the number of fluorescent molecules in the OVE that are observed as fluorescence intensity fluctuations (Figure 7B). If one considers a very short lag time (τ_s) compared to the average diffusion time of the molecule (τ_D) one can appreciate that the number of fluorescent molecules in the OVE is not very likely to change during τ_s . Therefore, $I(t)$ and $I(t + \tau_s)$ is likely very similar, thus the similarity between all analyzed τ_s lag times is very similar and consequently $G(\tau)$ is close to its maximum value (Figure 7C). In theory, $G(\tau)$ reaches its maximum at $\tau = 0$ and $G(0)$ is inversely proportional to the average number of fluorescent molecules in the OVE (176). By using different fitting models to describe the autocorrelation function from recorded data (assuming that the recorded intensity fluctuations are caused by free diffusion of molecules) it is possible to calculate the intercept with the y-axis which reports an estimate on the number of fluorescent molecules in the OVE. On the other hand, if one considers a very long lag time

(τ_L) compared to (τ_D), the number of fluorescent molecules in the OVE is not very similar, $I(t)$ and $I(t + \tau_L)$ are not correlated anymore and at $G(\tau_L)$ decays towards 0 (Figure 7B and C). The characteristic diffusion time of a molecule (τ_D) is defined by the lag time where $G(\tau)$ decays to its half-maximum value. From this analysis the primary experimental obtained parameters of a molecule are the number of particles in the OVE and τ_D . In order to quantitatively interpret FCS data, it is important to accurately adjust and calibrate the set-up before each set of experiments. Without going into details, calibration with a reference fluorophore is important to know the exact size and shape of the OVE in order to correctly calculate for example the diffusion coefficient of a molecule.

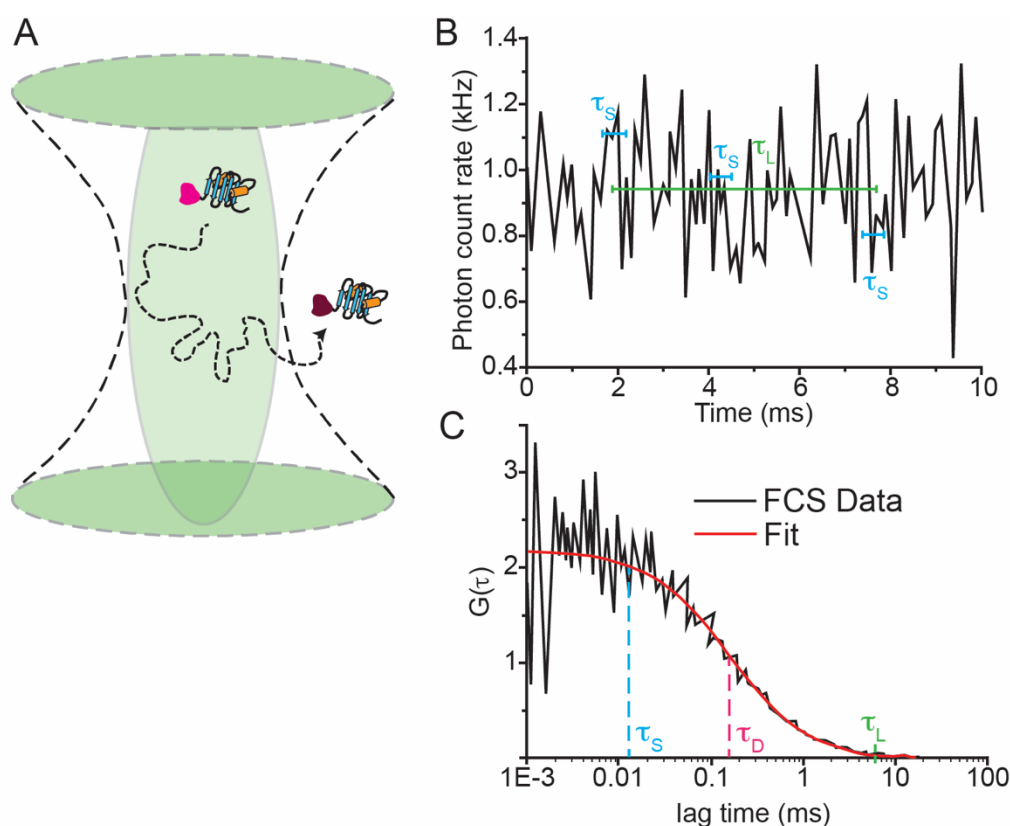


Figure 7: Overview of an FCS measurement. (A) An excited fluorescently labeled protein is diffusing through the confocal OVE. (B) Detected fluorescence intensity fluctuations due to the diffusion of fluorescently labeled molecules through the OVE (or due to the chemical properties of the fluorophore). (C) Characteristic decay of the autocorrelation function derived from the intensity fluctuations in B. Reproduced from Macháň *et al.* 2016 (175).

Probably the most important step in the analysis of FCS data is the choice of an appropriate fitting model for $G(\tau)$. The autocorrelation function in Figure 7C is a good example for a monodisperse system that has only one characteristic τ_D . However, samples can be more complex, as they can contain mixtures of free fluorophores and fluorophores bound to a protein, as well as two or more molecules that interact with each other. Consequently, the

autocorrelation function contains contributions from several diffusion times. Therefore, it is important to have some preliminary idea about the sample composition and how many parameters one would expect (*i.e.* deciding on the number of free parameters in the fitting function). Additionally, FCS data often has a low signal-to-noise ratio and correlated noise in $G(\tau)$. Another fact that one has to keep in mind is that $I(t)$ contributes with the square to $G(\tau)$. This means that the brightness of a relatively rare large particle (in comparison to the average particle) which contains several fluorophores strongly influence the shape of $G(\tau)$. In order to overcome the issue of overfitting of the data by “model picking” several quite complex methods have been developed in order to interpret FCS data more bias-free (177, 178).

Taken together, FCS is a very powerful tool that can be used to study the characteristic molecular properties and interactions of a molecule, peptide or protein but one has to be aware that a thorough calibration of the set-up and mindful data analysis is the foundation of a meaningful experiment.

4 RESULTS AND DISCUSSION

4.1 ASSEMBLY-FUNCTION RELATIONSHIP OF BRICHOS DOMAIN PROTEINS

As described in 1.3.3 ATP-independent molecular chaperones are diverse in their sequence, assembly size, and mechanism of action. Most of these chaperones are highly flexible and exist in dynamic equilibria between low- and high-affinity states for non-native or misfolded substrates, that shift in response to stress conditions (99). The proSP-C BRICHOS and Bri2 BRICHOS domains have been shown to interfere in the aggregation pathway of several substrates and are able to adopt various quaternary structures. Despite its high expression in brain tissue, the Bri3 BRICHOS domain has not been investigated regarding its quaternary structures and molecular chaperone functions. While the proSP-C BRICHOS domain forms mainly trimers in solution, Peng and co-workers observed already in 2010 HMW assemblies of Bri2 BRICHOS under non-reducing conditions, but did not investigate this finding in greater detail (111, 113, 161, 164). Therefore, we sought to get a more comprehensive understanding of the ability of the Bri2 BRICHOS domain to inhibit different types of protein aggregation in relation to its quaternary structure (paper I). Furthermore, we characterized the Bri3 BRICHOS domain in comparison with the Bri2 BRICHOS domain (paper IV).

4.1.1 Quaternary structures

Using the spider silk protein derived solubility tag NT* (179) enabled us to separate Bri2 BRICHOS monomers, dimers and large polydisperse oligomers (Paper I). More specifically, size exclusion chromatography (SEC) after removal of the solubility tag NT* reveals that Bri2 BRICHOS forms an equilibrium between monomers and non-covalently linked dimers. Furthermore, isolated covalently linked Bri2 BRICHOS dimers partially associate non-covalently into tetramers. Electron microscopy and SEC show that the Bri2 BRICHOS oligomers form well-structured particles consisting of 20 – 30 subunits with a dihedral (D2) symmetry and that the particles contain an even, but variable number of disulfide-linked subunits. A summary of different Bri2 BRICHOS assembly states are illustrated in Figure 8. The formation of large polydisperse oligomers ranging from 12 to more than 32 subunits with dimers as the basic building block is a feature that many classical sHSPs have in common (180-182). In contrast to the Bri2 BRICHOS domain, dimer association and oligomer assembly of sHSPs is likely not dependent on the formation of intermolecular disulfide bonds but rather non-covalent interactions of multiple regions within the molecular chaperone (183). These results show that there are some common basic features concerning the

quaternary structure that are similar between sHSPs and the Bri2 BRICHOS domain but also distinct differences. Furthermore, we found disulfide dependent HMW assemblies of the Bri2 BRICHOS domain in conditioned culture medium of a neuroblastoma cell line, a transfected human embryonic kidney cell line and after incubation of Bri2 BRICHOS monomers in mouse serum. The existence of different quaternary structures in these experiments indicate their potential physiological relevance. In the following descriptions Bri2 BRICHOS species refer to: oligomers (polydisperse HMW assemblies), dimers (mainly covalently linked dimers), monomers (monomers in equilibrium with some non-covalently linked dimers).

ATP-independent molecular chaperones are suggested to bind substrates through exposed hydrophobic surface areas. We show that Bri2 BRICHOS monomers, dimers and oligomers expose hydrophobic patches but more pronounced for Bri2 BRICHOS oligomers. The overall secondary structure of Bri2 BRICHOS monomers and dimers is similar to trimeric proSP-C BRICHOS that is characterized by a high content of random coil structures. In contrast, Bri2 BRICHOS oligomers appear to be somewhat more structured, indicating structural rearrangements upon assembly formation. In the light of these results, we speculated that there are differences in the efficiency of the Bri2 BRICHOS species to interfere with fibrillar or amorphous protein aggregation. Furthermore, in paper IV we found that unresolved preparations of the Bri2 BRICHOS domain and the Bri3 BRICHOS domain are very similar regarding their ability to form disulfide dependent HMW assemblies, secondary structure and surface hydrophobicity. However, in this study we used Trx as solubility tag and not NT*, and both BRICHOS domain constructs form almost exclusively large oligomers. We speculate that this observation might be related to the use of Trx as solubility tag and I will come back to this observation at the end of chapter 4.1.3.

4.1.2 Effects on protein aggregation and associated toxicity

In order to gain insights into how Bri2 BRICHOS monomers, dimers and oligomers as well as the unresolved preparation of Bri3 BRICHOS affect amyloid fibrillation we analyzed A β ₄₂ self-aggregation kinetics by the ThT fluorescence assay, as outlined in 1.1.5 and 3.2.2. Comparing the sigmoidal fitting parameters, aggregation half time ($\tau_{1/2}$) and maximum rate of aggregation (r_{\max}), revealed that the Bri2 BRICHOS dimer is the most efficient species followed by the monomer. It is important to mention that concentrations were calculated assuming monomeric protein solutions, which lowers the effective molecular ratio of *e.g.* Bri2 BRICHOS oligomers *vs.* monomers in the measurements. Especially, Bri2 BRICHOS oligomers exist in a broad range of assembly states and therefore it is difficult to correct the data for equal stoichiometries. Considering that the Bri2 BRICHOS dimer is more efficient,

despite a lower total number of molecules relative to monomers it was intriguing to speculate that the mechanism of action to delay A β ₄₂ fibrillation might vary between species. Applying a set of kinetic equations to extract the microscopic rate constants that can be used to describe A β ₄₂ growth curves revealed that all Bri2 BRICHOS species affect fibril-end elongation and secondary nucleation rate constants, and that the Bri2 BRICHOS dimer is most efficient on both parameters. Similarly, we found in paper IV that Trx-derived Bri3 BRICHOS proteins have effects on secondary pathways of A β ₄₂ aggregation.

Next, we determined the capacity of each Bri2 BRICHOS species to prevent the A β ₄₂-induced reduction of the γ oscillation power in hippocampal mouse brain slices. γ oscillations are linked to learning, memory and other higher cognitive processes, and changes have been shown in several disorders that are associated with cognitive impairment, like AD (184-186). In these experiments we used crude A β ₄₂ preparations (species < 30 kDa) and concentrations that are 60-fold lower compared to the concentrations we used in the bulk ThT fluorescence kinetic assay, where the first ThT positive aggregates are observed after about 30 minutes (starting from monomeric A β ₄₂ preparations). This time roughly corresponds to the incubation time of A β ₄₂ before the first γ oscillation recordings are performed. Lower A β ₄₂ concentrations result in longer lag phases and slower overall A β ₄₂ aggregation kinetics. Despite the fact that we used slightly different A β ₄₂ preparations one can assume that the A β ₄₂ mixture that is present at the start of the electrophysiological recording likely consist of a heterogeneous mixture of monomers, differently sized oligomers and prefibrillar aggregates but only a few fibrils. However, to get a better understanding about the structural properties of the A β ₄₂ species that evoke neurotoxicity, further studies should be conducted with the aim to establish the structural properties of these aggregates. Measuring γ oscillations in the presence and absence of different Bri2 BRICHOS species showed that all species reduce A β ₄₂-induced neurotoxicity and that Bri2 BRICHOS monomers are able to completely prevent toxic effects of A β ₄₂ at equimolar concentrations. Dimers and oligomers appear roughly equally efficient but even at a 2-fold molar excess of these BRICHOS species over A β ₄₂ they do not prevent toxicity as potently as Bri2 BRICHOS monomers.

Despite the difficulties to compare absolute numbers of Bri2 BRICHOS molecules due to their inherent heterogeneity, it is still appealing to speculate about the different outcomes in A β ₄₂ kinetic and toxicity experiments for dimers and monomers. Surprisingly, the size of a hypothetical Bri2 BRICHOS dimer (juxtaposing two monomers) could match the cross-sectional area of an experimentally solved mature A β ₄₂ fibril with a cross-beta sheet structure

with two A β ₄₂ molecules per fibril layer (187, 188). On the other hand, a Bri2 BRICHOS monomer fits with the cross-sectional area of a single-layer β -sheet that may exist in A β ₄₂ oligomers or prefibrillar aggregates. We hypothesized that Bri2 BRICHOS dimers are able to cover A β ₄₂ fibril surfaces and fibril-ends of mature fibrils more efficiently than Bri2 BRICHOS monomers and hence appear slightly more efficient in reducing the overall kinetics of A β ₄₂ fibrillation. Bri2 BRICHOS monomers on the other hand could bind to smaller oligomeric and protofibrillar A β ₄₂ aggregates diminishing their toxic effects on γ oscillations.

Previously, Bri2 BRICHOS preparations with unresolved assembly states have been shown to prevent non-fibrillar protein aggregation, similar to classical ATP-independent molecular chaperones (161). We followed the aggregation behavior of thermo-denatured CS in presence of different Bri2 BRICHOS species and found that exclusively Bri2 BRICHOS oligomers prevent amorphous protein aggregation. Furthermore, monomers that were incubated in serum whereby they form polydisperse oligomers are also potent in inhibiting CS from aggregation. This emphasizes that Bri2 BRICHOS oligomers with classical chaperone function can be formed under physiological conditions. Substrate-chaperone recognition sites and mechanisms of how ATP-independent molecular chaperones interact with different aggregates are still enigmatic but generally sHSPs have been shown to be less efficient in preventing larger proteins from aggregation, suggesting that the mass ratio is more important compared to the molar ratio (183). This could indicate that either non-native CS conformations and aggregates thereof are too big for Bri2 BRICHOS monomers and dimers or that Bri2 BRICHOS oligomers expose different binding sites than the monomers or dimers. We could not give further structural explanations about the specific substrate interaction sites of different Bri2 BRICHOS species, but the activation of Bri2 BRICHOS oligomers must go in line with structural rearrangements as observed by CD spectroscopy. Bri3 BRICHOS in comparison to unresolved Bri2 BRICHOS is similarly efficient in inhibiting non-fibrillar protein aggregation.

In summary, we demonstrated in paper I that we can isolate different Bri2 BRICHOS species, that monomers are very potent in inhibiting neuronal network toxicity originated from A β ₄₂, that dimers prevent A β ₄₂ fibrillation most efficiently and that exclusively HMW assemblies are very efficient inhibitors of non-fibrillar protein aggregation (Figure 8). The closely related Bri3 BRICHOS domain (79 % similar or identical residues) has very similar activities compared to mainly oligomeric Bri2 BRICHOS preparations, suggesting overlapping and potentially conserved molecular chaperone functions for the BRICHOS domains of the Bri

family (Figure 8). Interestingly, the proSP-C BRICHOS domain which forms mostly trimers and some monomers in solution has been shown to exclusively inhibit secondary nucleation pathways during A β ₄₂ fibril formation and associated neurotoxicity and has only very minor potency in preventing non-fibrillar aggregation (53, 161). These results indicate that the ability to prevent distinct substrates from aggregation might be encoded in the BRICHOS quaternary structure, but we will come back to that in chapter 4.1.3.

4.1.3 Bri2 BRICHOS assembly mechanism

The Bri2 BRICHOS domain is the ectodomain of the Bri2 protein that can be released into the extracellular space by proteolytic cleavage (135). In paper I we found Bri2 BRICHOS HMW assemblies in the conditioned culture medium of different cell lines and after incubation of monomers in serum. Bri2 BRICHOS oligomers are clearly the only potent species against non-fibrillar protein aggregation and contain a polydisperse mixture of disulfide-linked assembly states. The two Cys residues in Bri2 BRICHOS are highly conserved in the BRICHOS super family (112). The conditions that initiate structural and functional changes might be complex and several activation mechanisms have been reported for ATP-independent molecular chaperones, but for Cys containing chaperones the redox environment might be potentially important. Therefore, we asked ourselves in paper III if the Bri2 BRICHOS domain is a redox-regulated molecular chaperone domain.

We found that Bri2 BRICHOS monomers convert into polydisperse HMW assemblies under reducing conditions concomitant with activation of the ability to prevent non-fibrillar protein aggregation. The overall secondary structure and surface-exposed hydrophobic area of these reduction-induced Bri2 BRICHOS HMW assemblies are appealingly similar to isolated oligomers. Furthermore, assembly formation can be induced by shifting the redox equilibrium of physiological relevant redox regulators towards the reductive end of the spectrum. Strongly oxidizing conditions on the other hand have no influence on secondary or quaternary structures of Bri2 BRICHOS monomers and oligomers, do not compromise the ability of Bri2 BRICHOS oligomers to prevent amorphous protein aggregation or give rise to active Bri2 BRICHOS monomers. It is conceivable that molecular chaperone functions are upregulated under conditions that constitute compartment-specific stress to protein homeostasis. In this light it makes sense that proteins that exist in the net reducing cytosolic environment, like HSP33 or the two yeast peroxiredoxins PrxI and PrxII shift their equilibrium from the inactive towards their active molecular chaperone conformation in response to oxidative stress conditions (102, 189).

Many proteins in the oxidizing extracellular environment are stabilized by disulfide bonds making them potentially sensitive to reductive stress conditions (190). Even though reductive stress is less studied than oxidative stress, there are several papers linking reductive stress to serious human conditions like inflammation, cardiomyopathy with protein aggregation or AD (191-193). Therefore, we wondered if reductive stress conditions could lead to protein aggregation using an extracellular body fluid as model substrate. Surprisingly, serum proteins form non-fibrillar aggregates at elevated temperatures only in the presence of reductant, and Bri2 BRICHOS monomers, oligomers and α -crystallin can reduce this reduction-induced aggregation. It was a bit counterintuitive that isolated Bri2 BRICHOS oligomers appeared less efficient than monomers, but it is likely that reducing conditions will also give rise to aggregation of Bri2 BRICHOS oligomers that may affect chaperone activity. So far, we have shown in paper III that serum proteins are sensitive to reductive stress which is also a trigger for Bri2 BRICHOS monomers to form HMW assemblies with affinities towards non-fibrillar substrates. However, we could not show a redox cycling between monomers and oligomers as reported for other ATP-independent molecular chaperones (102, 189). This could either mean that we did not find the right conditions that would reduce disulfide bonds in the Bri2 BRICHOS oligomer and release smaller species or, as we speculate, that anti-amyloid active Bri2 BRICHOS monomers might constitute a reservoir in the extracellular space that can be activated upon reductive stress insults to chaperones that prevent non-fibrillar protein aggregation. Further studies will be needed to prove or disprove either of these hypotheses.

In order to get some further insights how Bri2 BRICHOS monomers convert into disulfide-dependent oligomers we investigated the activation mechanism in more detail, with regard to the redox state of the Cys residues. At first, we quantified free thiols in solution for all Bri2 BRICHOS species using the Ellman's reagent. As expected, we found that under native and denaturing conditions all thiols are engaged in either intramolecular (monomer) and/or intermolecular disulfide bonds (dimer and oligomer). We could also detect (as expected) two free thiols for completely reduced Bri2 BRICHOS monomers. Surprisingly, we could detect only one free thiol per molecule under denaturing and reducing conditions for Bri2 BRICHOS dimers and oligomers, indicating that one of two intermolecular disulfide bonds is resistant to complete reduction under the tested conditions. This was supported by the observation of a Bri2 BRICHOS dimer with one intermolecular disulfide even after incubation with a very high molar excesses of reductant, using polyacrylamide gel electrophoresis.

With the aim to assign the two Cys residues, namely Cys164 and Cys223 to specific disulfide bonds with apparently distinct reduction potentials we first used a proteomics MS set-up as outlined in 3.1.2. We were able to assign peptide fragments containing the Cys164-Cys164 homodisulfide or Cys164-Cys223 heterodisulfide bonds in all fractions (monomers, dimers, oligomers) under non-reducing conditions and concluded that the absence of detection of the Cys223-Cys223 heterodisulfide bond in MS experiments is due to a high density of repelling charges in this peptide fragment. Using the same set-up but under reducing conditions, we could find peptide fragments for both Cys residues in Bri2 BRICHOS monomer fractions. Interestingly, in Bri2 BRICHOS dimer and oligomer fractions only the Cys164 containing peptide fragment is present. The lack of success to detect the Cys223 in dimer and oligomeric fractions can have two reasons. Either there are structural differences in comparison to monomers that do not allow equivalent proteolytic cleavage, or the homodisulfide bond Cys223-Cys223 is resistant towards full reduction. We concluded from these results that heterodisulfide bonds (that must occur in Bri2 BRICHOS monomers) as well as homodisulfide bonds, are formed in different Bri2 BRICHOS assembly states and that our data points to the Cys223-Cys223 homodisulfide bond as the more stable disulfide. Furthermore, single Cys to Ser substitution mutants show that Cys223-Cys223 dimers are more stable compared to Cys164-Cys164 dimers and mixing of mutants with and without the solubility tag linked for detection purposes, suggested that the disulfide bond in Cys223-Cys223 linked dimers are able to swap between subunits.

Altogether, we established in paper III that Bri2 BRICHOS monomers are able to convert into chaperone active polydisperse HMW assemblies (Figure 8). We concluded that cycles of reduction and re-oxidation of intra- and intermolecular homodisulfide bonds are mediated by distinct thiol reactivities, whereby the Cys223-Cys223 homodisulfide bond is key to the stability of the dimeric substructure. Furthermore, we speculate that shifting the equilibrium towards Bri2 BRICHOS oligomers in response to reductive stress conditions in the net oxidizing extracellular environment could contribute to protect the organismal homeostasis.

In the end, I would like to shortly refer back to our observation that we almost exclusively find Bri2 BRICHOS and Bri3 BRICHOS oligomers in purifications using the Trx-tag. Generally cytosolic protein expression in *E. coli* occurs in a reducing environment and we used in both studies (paper I and IV) the same *E. coli* strain. The physiological redox regulators that we found to mediate the formation of Bri2 BRICHOS oligomers from monomers include also the Trx system. Furthermore, the Trx solubility tag contains the catalytic CXXC motif which might be activated (reduced) in the reducing cytosolic

environment. Using the Trx tag as solubility tag for protein expression will increase the overall cytosolic Trx concentration and the Trx-BRICHOS fusion protein will create a very high local concentration due to the intramolecular arrangement. One can speculate that this environment will shift the equilibrium of the redox sensitive Bri2 BRICHOS and Bri3 BRICHOS domain even more towards large oligomers in comparison to the redox-inert NT*-tag.

4.2 MODULATION OF THE PROSP-C BRICHOS AND BRI2

BRICHOS ASSEMBLY STATE AND ANTI-AMYLOID ACTIVITY

ProSP-C BRICHOS and Bri2 BRICHOS share ~25% identical residues or conservative replacements but their subunit overall secondary and tertiary structure are predicted to be largely conserved (112, 162). While the proSP-C BRICHOS domain forms mainly non-covalently linked trimers (111), Bri2 BRICHOS exists as monomers and disulfide-dependent polydisperse assemblies. Introducing a serine to arginine (Arg) mutation in the trimer interface of proSP-C BRICHOS shifts the equilibrium towards monomers and increases the efficiency to inhibit A β ₄₂ fibril formation (157). However, we recognized a threonine (Thr) at position 187 in the proSP-C BRICHOS trimer interface that pokes into a positively charged pocket on the neighboring subunit (Figure 6C), which corresponds to Arg221 at the homologous position in a structural model of Bri2 BRICHOS.

In paper II and V we introduced mutations in the Bri2 BRICHOS (Arg 221 to glutamic acid (R221E)) and proSP-C BRICHOS domains (Thr 187 to Arg (T187R)), respectively, with the aim to create repulsions between the subunits by modulating the respective surface charge of the subunits. MS as well as other complementary methods showed that proSP-C BRICHOS T187R forms stable monomers and Bri2 BRICHOS R221E shifts the Bri2 BRICHOS assembly spectrum towards smaller species but disulfide dependent dimers and polydisperse oligomers still exist. However, upon incubation, Bri2 BRICHOS R221E oligomers appear to be less stable compared to WT oligomers. Notably, the equilibrium between monomers and non-covalently linked dimers that we find for WT Bri2 BRICHOS is completely shifted towards the monomer for Bri2 BRICHOS R221E, even at high BRICHOS concentrations. Mixing of monomeric R221E with WT oligomers, destabilizes WT oligomers that subsequently release smaller subunits. Since polydisperse WT Bri2 BRICHOS oligomers are characterized by inter-subunit disulfide bonds, it is reasonable that the presence of R221E monomers will not be enough to fully dissociate them into small species.

Both mutants suppress A β ₄₂ fibril formation in sub-stoichiometric concentrations and almost exclusively inhibit secondary nucleation events. In paper I, WT Bri2 BRICHOS monomers prevented secondary nucleation but also to some degree A β ₄₂ fibril end-elongation. Since monomeric WT fractions contain also non-covalently linked dimers, which R221 monomer fractions do not, our results corroborate that BRICHOS monomers are the most efficient species in blocking secondary nucleation events and hence have the greatest potential to prevent neurotoxic effects of small fibril surface-catalyzed A β ₄₂ aggregates. Accordingly, Bri2 BRICHOS R221E monomers most efficiently prevent A β ₄₂ induced neurotoxicity in hippocampal mouse brain slices. In line with our postulated model in paper I, Bri2 BRICHOS R221 dimers affect fibril end-elongation, in addition to secondary nucleation. Moreover, we demonstrate that the release of smaller subunits from Bri2 BRICHOS oligomers by Bri2 BRICHOS R221E monomers enhances their overall efficiency to prevent A β ₄₂-derived neurotoxic effects, providing a possible way to modulate the anti-A β ₄₂ capacity of the PN (Figure 8).

Turning to proSP-C BRICHOS it was previously hypothesized that the proSP-C BRICHOS monomer is the active conformation and the trimer acts as an inactive storage conformation where the proposed A β binding site, face A, is inaccessible (157). However, in paper V we found some challenging results, showing that at low concentrations the purely monomeric proSP-C BRICHOS T187R mutant is equally efficient in preventing the overall rate of A β ₄₂ aggregation compared to the WT after correcting for the molecular stoichiometry. However, the sigmoidal fitting parameters $\tau_{1/2}$ and r_{max} saturate for high BRICHOS concentrations at lower levels for the WT. Both, proSP-C BRICHOS T187R monomers and WT trimers bind to immobilized A β ₄₂ fibrils but the mutant monomer binds with an apparent 5-fold higher affinity as measured by surface plasmon resonance spectroscopy (SPR). This demonstrates that both, proSP-C BRICHOS monomers and trimers, can interact with A β ₄₂ and prevent its self-aggregation. We speculated that the proSP-C BRICHOS trimer might expose another binding site with lower affinity for A β ₄₂ fibrils compared to the monomer. However, structural investigation of proSP-C BRICHOS bound to A β ₄₂ fibrils will be needed to prove this hypothesis.

4.3 PROSP-C BRICHOS AS A TOOL TO STUDY AMYLOID FORMATION

A recent study proposed that A β ₄₂ fibril proliferation occurs through a two-step nucleation mechanism where first A β ₄₂ monomers form small unstable oligomers that can dissociate

back to monomers. However, these oligomers eventually convert into an A β ₄₂ oligomer that can grow into mature fibrils (converting oligomer). Using mathematical modeling it was estimated that the converting oligomers roughly consist of 4 – 9 A β ₄₂ monomers (194). After establishing that proSP-C BRICHOS T187R forms pure and stable monomers and strongly prevents secondary nucleation events we wondered if we could use this proSP-C BRICHOS variant to study binding towards small A β ₄₂ aggregates by FCS.

We used an amine-reactive dye to label proSP-C BRICHOS T187R under conditions where only a fraction of all proteins is labeled and essentially carry only one dye molecule per protein. It is important to ensure that the binding abilities of proSP-C BRICHOS T187R are not compromised by multiple labeling with fluorophores. FCS and fluorescence cross-correlation spectroscopy (FCCS) experiments show that proSP-C BRICHOS T187R does not bind to A β ₄₂ monomers. This was confirmed by SPR spectroscopy measurements where no binding towards immobilized A β ₄₂ monomers was detected, which is similar to WT proSP-C BRICHOS (53).

To determine binding of proSP-C BRICHOS to small A β ₄₂ aggregates we followed the A β ₄₂ aggregation over time in presence of proSP-C BRICHOS T187R using FCCS and analyzed the autocorrelation curves and cross-correlation curves using the maximum entropy method for FCS. This method is a fitting routine that was developed for a more bias-free interpretation of autocorrelation curves with multiple components, which was necessary since A β ₄₂ aggregation is inherently heterogeneous. FCS and FCCS data reveal that proSP-C BRICHOS T187R binds to a heterogeneous mixture of soluble A β ₄₂ aggregates of increasing sizes over time and that multiple BRICHOS molecules are able to bind to A β ₄₂ aggregates as they grow in size. Nonetheless, in our FCCS experiments we also found a distribution of diffusion times that represent small A β ₄₂ aggregates that are bound by one labeled proSP-C BRICHOS T187R molecule. Unfortunately, we cannot resolve this diffusion time from the average diffusion time of a free proSP-C BRICHOS T187R molecule (not bound to A β ₄₂). The reason is that in FCS the diffusion time of spherical molecules scales with the third power of the molecular weight. However, the FCCS data shows that these small aggregates must contain one labeled proSP-C BRICHOS T187R molecule and at least one labeled A β ₄₂ molecule and several unlabeled A β ₄₂ monomers. We calculated that our resolution limit lies below a theoretical A β ₄₂ aggregate made up of less than 9 monomers. Since proSP-C BRICHOS T187R does not bind to A β ₄₂ monomers, has no effects on primary nucleation but inhibits secondary nucleation we concluded that these small (< 9 monomers) A β ₄₂ aggregates

must be secondary nucleation competent (Figure 8). This size range fits surprisingly well with the upper limit of the proposed converting oligomers (194). The trimeric WT proSP-C BRICHOS domain has been recently extensively used to advance the kinetic description of A β ₄₂ aggregation (171, 194-196). In this light, we believe that the purely monomeric and ATP-independent proSP-C BRICHOS T187R mutant is a good complementary molecular model chaperone to study the kinetics of various amyloidogenic peptides in molecular detail.

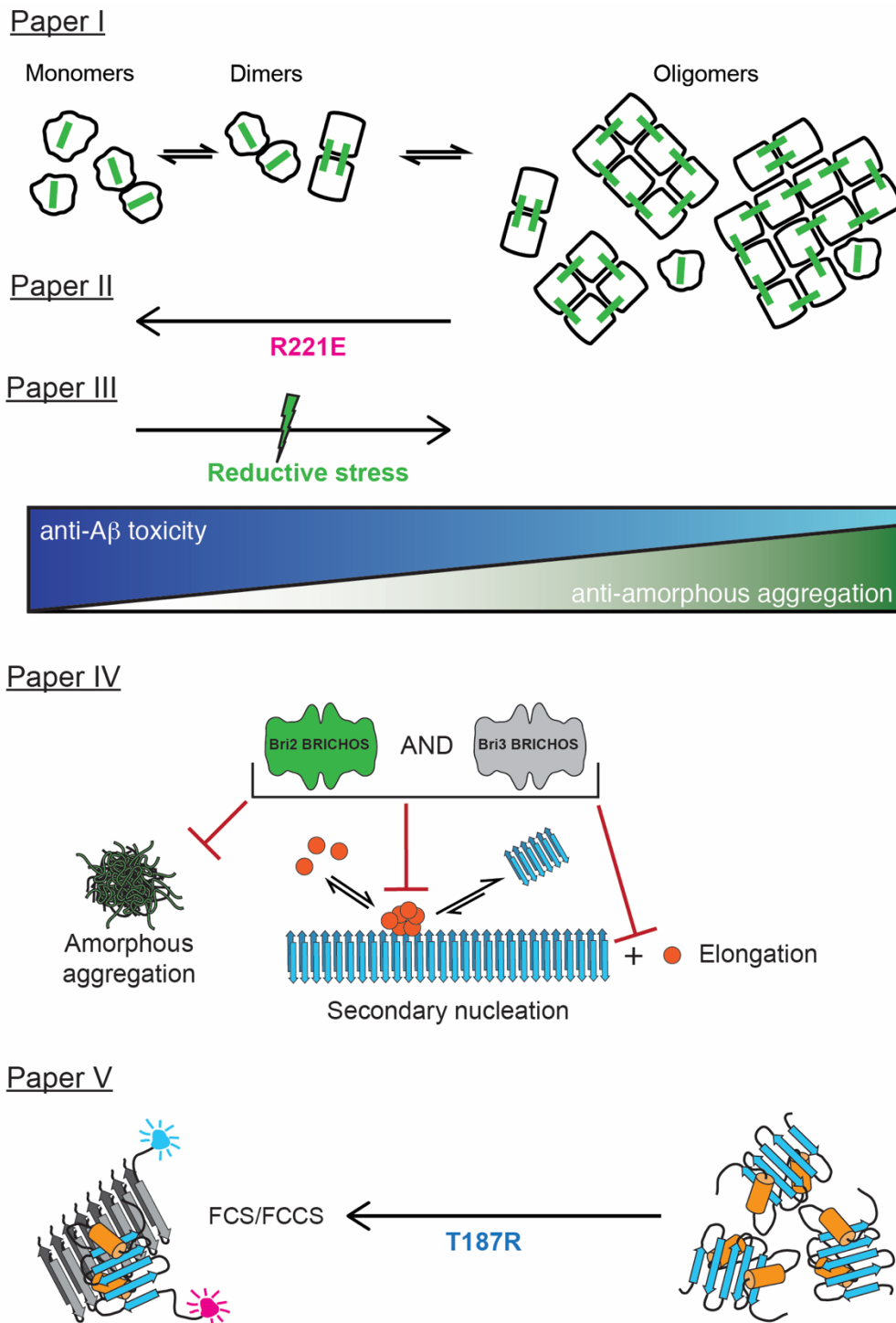


Figure 8: Graphical summary of the work presented in this thesis. The Bri2 BRICHOS domain can form monomers, dimers and disulfide-linked polydisperse oligomers and the assemblies differ in their activities to prevent A β_{42} -induced neuronal network toxicity or amorphous protein aggregation (paper I). The monomeric Bri2 BRICHOS R221E mutant is able to partly disassemble WT BRI2 BRICHOS oligomers with enhanced effects to prevent A β_{42} -induced toxicity (paper II). Bri2 BRICHOS monomers convert into disulfide-dependent oligomers under reducing conditions (paper III). HMW preparations of Bri2 and Bri3 BRICHOS are very similar in their abilities to prevent non-fibrillar protein aggregation, secondary nucleation on amyloid fibrils and amyloid fibril end-elongation (paper IV). The monomeric proSP-C BRICHOS T187R mutant enabled us to detect binding towards small secondary nucleation competent A β_{42} aggregates (paper V).

5 CONCLUSIONS AND FUTURE PERSPECTIVES

In this thesis, we have presented insights into the abilities of BRICHOS domains from different proproteins to prevent fibrillar and non-fibrillar protein aggregation and demonstrated an assembly specific substrate specificity for the Bri2 BRICHOS domain. Furthermore, we show that exclusively Bri2 BRICHOS oligomers possess molecular chaperone functions to prevent non-fibrillar protein aggregation and are generated from monomers under reducing conditions. Surprisingly, under similar conditions serum proteins form insoluble non-fibrillar aggregates. We propose that the recruitment of Bri2 BRICHOS monomers to form HMW assemblies could be a way to boost the extracellular PN and maintain homeostasis upon reductive stress.

From our observations that BRICHOS monomers are the most efficient species in blocking the generation of toxic nuclei catalyzed at the surface of already formed amyloid fibrils, we were able to design a Bri2 BRICHOS monomer mutant with the ability to partly disassemble Bri2 BRICHOS oligomers that show enhanced anti-amyloid activities. We speculate that these findings harness the possibility to increase the anti-amyloid capacity of the PN in amyloid-associated disorders by activating endogenous Bri2 BRICHOS oligomers.

Furthermore, we generated a stable proSP-C BRICHOS monomer mutant by introducing a mutation at the homologous position compared to Bri2 BRICHOS. This mutant enabled us to show binding of a proSP-C BRICHOS monomer to small but yet secondary nucleation competent, supposedly toxic, $A\beta_{42}$ aggregates with an estimated size of less than nine monomers by FCS. We hypothesize that the high efficiency of the proSP-C BRICHOS domain to reduce $A\beta_{42}$ aggregation-associated toxicity (53) is reflected by the ability to bind to the smallest secondary nucleation competent $A\beta_{42}$ aggregates.

Even though we could unravel several features of the molecular chaperone domain BRICHOS there are still many open questions. For example, we show a 3D density map of a Bri2 BRICHOS oligomer, however, there is still little known about the structural changes that occur during the conversion from monomers to oligomers or about the potential substrate binding sites. Additionally, the physiological relevance under basal and/or stress conditions of each Bri2 BRICHOS species remains to be established. Furthermore, the proSP-C BRICHOS monomer was suggested to be the anti-amyloid active conformation while the trimer is inactive (157). However, we could detect binding of the proSP-C BRICHOS trimer to $A\beta_{42}$ fibrils (with 5-fold lower affinity) and similar effects on $A\beta_{42}$ aggregation kinetics

compared to the monomer mutant. This raises the questions if the trimer is able to expose face A, at least in one subunit or if there is a face A independent binding site for A β ₄₂ fibrils.

ATP-independent molecular chaperones are rather “holdases” than “foldases” and it remains to be seen how they sequester misfolded or aggregated proteins in the extracellular space. Since the extracellular environment has only low levels of ATP it is unlikely that secreted ATP-dependent molecular chaperones would take on this task. Some studies show that scavenger and lipoprotein receptors mediate the internalization of misfolded and aggregated proteins and that they are less toxic if they are taken up in complexes with molecular chaperones (197, 198). Interestingly, recombinant Bri2 BRICHOS that has been delivered to the mouse brain by focused ultrasound is taken up by a subset of neurons (199). We found that Bri3 BRICHOS behaves very similar in terms of quaternary structure and function compared to Bri2 BRICHOS but shedding of the ectodomain has not been reported. One appealing hypothesis could be that membrane-bound Bri3 BRICHOS co-oligomerizes with other secreted BRICHOS domains and functions as a BRICHOS specific receptor. Likewise, it is imaginable that regulation of Bri2 cleavage under normal and stress conditions can shift the equilibrium between membrane-bound and secreted Bri2 BRICHOS, making it a self-regulated chaperone-receptor.

Taken together, we outlined some basic principles of the structure-function relationship of the BRICHOS domain and paved the way for further investigations regarding the identification of substrate binding sites, extracellular chaperone functions and potential applications in aggregation disorders.

6 ACKNOWLEDGMENTS

My doctoral thesis is the summary of a 5 year-long journey that would not have been as successful or as much fun without numerous people and therefore I am really thankful!

First of all, I would like to thank my main supervisor **Janne** for making me part of your fabulous group and for believing in me as a scientist – and person, I hope. The inspiring and calm atmosphere you create makes work very enjoyable and most productive, as I believe. I'm grateful for your open ears and support of any of my ideas and your ability to make weeklong failures and negative results feel not so bad by commenting them with “At least now we know!” ☺. Your sharp mind and ability to keep up with all projects in the group but still finding the time to discuss even the tiniest problems is impressive – So keep up the good work! You are definitely an inspiration for my future.

I would also like to thank my co-supervisors Henrik & Jenny that were especially guiding me when it came to the many very basic problems during a PhD, like “Is there a desk for me?”, “The Äkta makes funny noises...”, or “The autoclave is broken – but I still need medium for my cells.”. **Jenny**, thank you very much for your positive attitude, enthusiasm in science and support of all my ideas which gives a baby PhD student a good amount of confidence. **Henrik** you joined the Axel maintenance team a bit later, but it just made sense since you anyway were my special lab supervisor when I needed help with instruments or quick protocol fixes. It is amazing how many different and probably unconventional methods you are willing to test – of which many might not work – and still would be positive and comment failures with a laugh!

Not listed as an official supervisor but basically in the team, I would like to thank you, **Gefei**, for guiding me already as a master student and mentoring me ever since. Something that I will always remember is when we stayed late in the lab because you proposed preparing a ThT assay at 6 pm claiming “Janne wants to know!” – I still don't know if he really needed to know the results the next morning... ;). Besides all the work I had a great time playing and discussing football with you!

Hannes: Thank you for being my mentor and basically initiating my PhD studies by bringing me to Sweden since you didn't know any protein related research group in Norway (but a nice one in Sweden!). I always enjoyed coming back to Würzburg for a coffee or a Christmas party!

Médoune it was amazing living 4 years with you... others might claim it was a 4 year-long marriage but what do they know! I could definitely not have imagined a better flat-mate and even if it is not super obvious, but my FIFA skills definitely improved from extremely bad to lousy... or was it the other way around?!

I would also like to thank the past and present JJ and AR group for a marvelous working atmosphere and help whenever needed! **Anna** for giving me the once in a lifetime chance to see and actually feed freaking huge spiders. **Kerstin** for sharing your enormous knowledge and solving cloning issues in the blink of an eye! Your lab organizing skills are just perfect and made work so much easier! Also, thank you that I cannot forget your smiling face when Germany got eliminated after the group stage during the World Cup 2018. **Oihan & Helen** you were the first ones I went for drinks with once I arrived in Sweden and I have to say it was quite an amazing internship with all the non-scientific activities! Thank you, **Simone** for all the life-lessons, introduction to Sardinian swearphrases and for dragging me to the dark side of science... the Western blot. **Lisa D** for good discussions and help in the lab. **Axel A** for persistently taking time explaining me your great fitting knowledge. Also, for an amazing lecture in all kinds of baby-related bureaucratic issues. To **Nina** for teaming up in a super well-organized, straight forward fashion to set up new protocols and giving the lab just a warm atmosphere. **Tina** for listening to my bad German word jokes. **Lorena** and **Juanita** for making the lunch time more enjoyable. **Urmi, Sameer & Soophie** for the basically never-ending good mood in our little office corner. To **Shaffi, Olga, Nina S.** and **Rakesh**, to complete the great atmosphere that you bring to the whole group(s). **Lovisa** and **Carlos** for being such awesome students on which I was allowed to practice my teaching skills ;).

Collaborators in other places: **Michael** for enthusiastically sharing all of your results and ideas like a lightning bolt, and for including me in several of your amazing projects. **Danai** for constantly helping me with the mass spectrometry experiments and looong conversations during incubation coffee breaks. **Ann & Vladana** for a fantastic collaboration and for accommodating me so kindly in your group. **Cecilia** for helping me with the CD experiments at your lab at SU, that I desperately needed, and nice conversations. And all other collaborators for fruitful projects and conversations.

Many thanks to Maria R., Eva, Helena and Maria A. for your help with various tasks and kindness, and everyone else working at NVS for all the support during my PhD studies.

Thanks a lot, to all my friends and fellow PhD students that make everyday life just better! **Dani** for giving me countless history lectures about the Bermuda Triangle on land: Portugal, Spain and the Basque country. Also, for giving my Friday evenings a purpose! **Raul** for all the jokes, laughs, movie references that I don't get and becoming our family photographer. To **Emilka** for your great everlasting enthusiasm in basically everything and the constant supply of polish T-shirts. **Martin** for bringing me closer to the world of the fancy beers and philosophizing about the handball skills of our team ("Make Hellas great again!"). **Amit & Mona** for so many things that are hard to list here... I'll tell you during our next coffee walks ;). To **Bernie** for just being the person you are and all the twisted conversations that are definitely an extraordinary training for the mind! To **Luis** the pizzaiolo with the cowboy hat for food, laughs and barrels of real tequila. **Nuno & Giacomo** for showing me how to behave like a queen, princess, or was it duchess...? To **Kirsten**, without you I would have never gone to the gym at 7 am in the morning! **Hazal** for showing me the potential flexibility of a spine that I could have never imagined. **Laetitia** for sharing all the amazing Amit food pictures with me. **Francesca, Andrea** (the second family photographer!), **Ceren, Lea, Ying, Yuniesky, Gorka** (I'll never forget your face after you dissected a whole day fly brains ☺), **Susana (2x), Joana, Chenhong, Marloes, Ipsit, and Maria (Gr)** for all the little everyday jokes that make days better. **Tom** for founding and maintaining our little Sunday league football. **Leo** for the scars on my legs. To **Teun** for sharing my sense of humor even though I'm sometimes not sure if people around us want to hear these jokes... And the rest of the **Football gang** for our fabulous games and giving my brain a rest ☺!

Natürlich auch Danke an meine Freunde daheim, für die grandiosen letzten 30 Jahre! **Frank**, den besten Metzger der Welt für herausragende Haxen und Heiligabendhäppchen. **Johannes** für überragende Konzertbesuche, Männerausflüge und alles andere was man mit 16 so macht ;). **Max** und **Lisa** dafür, dass ihr mich daheim immer so herzlich willkommen heißt und mich die Heimat wirklich vermissen lasst. Und natürlich kommt das Letzte zum Schluss, vielen Dank **Fabi** du geschmeidiger Mollusk für eine verdammt geile Studienzeit (ich lass die Details weg) und dass ich bei dir immer ein Bett und einen Kater frei hab!

Ich möchte mich auch bei meiner Familie, **Mama, Papa, Oma-Rola, Opa-Fritz, Heike, Momele & Magger** für die langjährige Unterstützung bedanken und dass ich mich daheim immer direkt wohl fühle – quasi wie, wenn ich nie weg war ☺. Vielen Dank an meine Eltern, die mich ja jetzt doch schon das ein oder andere Jahr durchfüttern mussten, aber mich immer bei allem unterstützt haben! Okay vielleicht nicht als ich mein Biostudium abrechnen wollte ;). Danke auch an den ganzen **Bunz-Clan** dafür, dass ihr mich so liebevoll bei euch

aufgenommen habt. To **Julen** (“Yes, yes!” – you appear in this section now ☺) for sharing all your (most of the time) hilarious analogies, Raul imitations and “Hold on, hold on, hold on” just being an amazing good friend. **Maria** you basically got dragged into this section with Julen and will forever be part of it. Thank you for your warm personality and counterbalancing of Julen when he becomes a bit too ecstatic. I’m really looking forward to your babysitting skills!

Zum Schluss, **Jessy** es ist schwer auszudrücken wie glücklich ich sein kann, dich zu haben und dass du mir nach Schweden gefolgt bist! Dafür, dass du mich immer zum Lachen bringst, mir den Rücken freihältst, wenn ich mal wieder länger brauche, an meiner Doktorarbeit rumfummle, beim Fußball bin oder auf Männerurlaub! Ich freue mich schon auf die nächsten Jahrhunderte mit dir und der **Marla**!

7 REFERENCES

1. Piovesan A, Antonaros F, Vitale L, *et al.* (2019) Human protein-coding genes and gene feature statistics in 2019. *BMC Res Notes* 12(1):315.
2. Malkov SN, Zivkovic MV, Beljanski MV, *et al.* (2008) A reexamination of the propensities of amino acids towards a particular secondary structure: classification of amino acids based on their chemical structure. *J Mol Model* 14(8):769-775.
3. Dill KA. (1990) Dominant forces in protein folding. *Biochemistry* 29(31):7133-7155.
4. Eden E, Geva-Zatorsky N, Issaeva I, *et al.* (2011) Proteome Half-Life Dynamics in Living Human Cells. *Science* 331(6018):764-768.
5. Kubelka J, Hofrichter J & Eaton WA. (2004) The protein folding 'speed limit'. *Curr Opin Struct Biol* 14(1):76-88.
6. Anfinsen CB, Haber E, Sela M, *et al.* (1961) Kinetics of formation of native ribonuclease during oxidation of reduced polypeptide chain. *Proc Natl Acad Sci U S A* 47(9):1309-1314.
7. Anfinsen CB. (1973) Principles that govern the folding of protein chains. *Science* 181(4096):223-230.
8. Levinthal C. (1969) How to fold graciously. *Mossbauer Spectroscopy in Biological Systems Proceedings* 67(41):22-24.
9. Kim PS & Baldwin RL. (1982) Specific intermediates in the folding reactions of small proteins and the mechanism of protein folding. *Annu Rev Biochem* 51:459-489.
10. Baldwin RL. (1989) How does protein folding get started? *Trends BiochemSci* 14(7):291-294.
11. Daggett V & Fersht AR. (2003) Is there a unifying mechanism for protein folding? *Trends BiochemSci* 28(1):18-25.
12. Bryngelson JD, Onuchic JN, Socci ND, *et al.* (1995) Funnels, pathways, and the energy landscape of protein folding: A synthesis. *Proteins-Structure Function and Bioinformatics* 21(3):167-195.
13. Ohgushi M & Wada A. (1983) 'Molten-globule state': a compact form of globular proteins with mobile side-chains. *FEBS Lett* 164(1):21-24.
14. Sali A, Shakhnovich E & Karplus M. (1994) How does a protein fold? *Nature* 369(6477):248-251.
15. Baldwin RL. (1994) Protein folding: Matching speed and stability. *Nature* 369(6477):183-184.
16. Dill KA & MacCallum JL. (2012) The Protein-Folding Problem, 50 Years On. *Science* 338(6110):1042-1046.

17. Hartl FU, Bracher A & Hayer-Hartl M. (2011) Molecular chaperones in protein folding and proteostasis. *Nature* 475(7356):324-332.
18. Pollard TD. (1990) Actin. *Curr Opin Cell Biol* 2(1):33-40.
19. Truscott RJW. (2005) Age-related nuclear cataract—oxidation is the key. *Exp Eye Res* 80(5):709-725.
20. Glenner GG & Wong CW. (1984) Alzheimer's disease and Down's syndrome: Sharing of a unique cerebrovascular amyloid fibril protein. *Biochem Biophys Res Commun* 122(3):1131-1135.
21. Yoshimura Y, Lin Y, Yagi H, *et al.* (2012) Distinguishing crystal-like amyloid fibrils and glass-like amorphous aggregates from their kinetics of formation. *Proc Natl Acad Sci U S A* 109(36):14446-14451.
22. Kampinga HH & Bergink S. (2016) Heat shock proteins as potential targets for protective strategies in neurodegeneration. *The Lancet Neurology* 15(7):748-759.
23. De Strooper B, Vassar R & Golde T. (2010) The secretases: enzymes with therapeutic potential in Alzheimer disease. *Nat Rev Neurol* 6(2):99-107.
24. Wright GSA, Antonyuk SV & Hasnain SS. (2019) The biophysics of superoxide dismutase-1 and amyotrophic lateral sclerosis. *Q Rev Biophys* 52:e12.
25. Vendruscolo M & Dobson CM. (2005) Towards complete descriptions of the free-energy landscapes of proteins. *Philos Trans R Soc* 363(1827):433-450.
26. Song JX. (2009) Insight into "insoluble proteins" with pure water. *FEBS Lett* 583(6):953-959.
27. Weids AJ, Ibstedt S, Tamas MJ, *et al.* (2016) Distinct stress conditions result in aggregation of proteins with similar properties. *Sci Rep* 6:24554.
28. Horwitz J, Huang QL, Ding LL, *et al.* (1998) Lens alpha-crystallin: Chaperone-like properties. *Molecular Chaperones* 290:365-383.
29. Roberts CJ. (2007) Non-native protein aggregation kinetics. *Biotechnol Bioeng* 98(5):927-938.
30. Philo JS. (2006) Is any measurement method optimal for all aggregate sizes and types? *Aaps Journal* 8(3):E564-E571.
31. Silow M & Oliveberg M. (1997) Transient aggregates in protein folding are easily mistaken for folding intermediates. *Proc Natl Acad Sci U S A* 94(12):6084-6086.
32. Michaels TCT, Saric A, Habchi J, *et al.* (2018) Chemical Kinetics for Bridging Molecular Mechanisms and Macroscopic Measurements of Amyloid Fibril Formation. In: Johnson MA, Martinez TJ, editors. *Annual Review of Physical Chemistry, Vol 69*. Annual Reviews. p. 273-298.
33. Eisenberg D & Jucker M. (2012) The amyloid state of proteins in human diseases. *Cell* 148(6):1188-1203.

34. Kollmer M, Close W, Funk L, *et al.* (2019) Cryo-EM structure and polymorphism of A beta amyloid fibrils purified from Alzheimer's brain tissue. *Nat Commun* 10:8.
35. Fändrich M. (2012) Oligomeric intermediates in amyloid formation: structure determination and mechanisms of toxicity. *J Mol Biol* 421(4-5):427-440.
36. Sipe JD & Cohen AS. (2000) Review: History of the amyloid fibril. *J Struct Biol* 130(2-3):88-98.
37. Pham CLL, Kwan AH & Sunde M. (2014) Functional amyloid: widespread in Nature, diverse in purpose. In: Perrett S, editor. *Amyloids in Health and Disease*. Portland Press Ltd. p. 207-219.
38. Dobson CM. (1999) Protein misfolding, evolution and disease. *Trends BiochemSci* 24(9):329-332.
39. Chiti F & Dobson CM. (2017) Protein Misfolding, Amyloid Formation, and Human Disease: A Summary of Progress Over the Last Decade. In: Kornberg RD, editor. *Annual Review of Biochemistry, Vol 86*. Annual Reviews. p. 27-68.
40. Jackson MP & Hewitt EW. (2017) Why are functional amyloids non-toxic in humans? *Biomolecules* 7(4):13.
41. Sipe JD, Benson MD, Buxbaum JN, *et al.* (2016) Amyloid fibril proteins and amyloidosis: chemical identification and clinical classification International Society of Amyloidosis 2016 Nomenclature Guidelines. *Amyloid* 23(4):209-213.
42. Sunde M, Serpell LC, Bartlam M, *et al.* (1997) Common core structure of amyloid fibrils by synchrotron X-ray diffraction. *J Mol Biol* 273(3):729-739.
43. Fitzpatrick AW, Debelouchina GT, Bayro MJ, *et al.* (2013) Atomic structure and hierarchical assembly of a cross-beta amyloid fibril. *Proc Natl Acad Sci U S A* 110(14):5468-5473.
44. Baldwin AJ, Knowles TPJ, Tartaglia GG, *et al.* (2011) Metastability of native proteins and the phenomenon of amyloid formation. *J Am Chem Soc* 133(36):14160-14163.
45. Törnquist M, Michaels TCT, Sanagavarapu K, *et al.* (2018) Secondary nucleation in amyloid formation. *Chem Commun (Camb)* 54(63):8667-8684.
46. Hardy J & Selkoe DJ. (2002) The amyloid hypothesis of Alzheimer's disease: Progress and problems on the road to therapeutics. *Science* 297(5580):353-356.
47. Hellstrand E, Boland B, Walsh DM, *et al.* (2010) Amyloid beta-protein aggregation produces highly reproducible kinetic data and occurs by a two-phase process. *ACS Chem Neurosci* 1(1):13-18.
48. Kurouski D, Dukor RK, Lu XF, *et al.* (2012) Normal and reversed supramolecular chirality of insulin fibrils probed by vibrational circular dichroism at the protofilament level of fibril structure. *Biophys J* 103(3):522-531.
49. Ferrone FA, Hofrichter J & Eaton WA. (1985) Kinetics of sickle hemoglobin polymerization II. A double nucleation mechanism. *J Mol Biol* 183(4):611-631.

50. Arosio P, Knowles TP & Linse S. (2015) On the lag phase in amyloid fibril formation. *Phys Chem Chem Phys* 17(12):7606-7618.
51. Cohen SIA, Vendruscolo M, Dobson CM, *et al.* (2012) From macroscopic measurements to microscopic mechanisms of protein aggregation. *J Mol Biol* 421(2-3):160-171.
52. Cohen SI, Linse S, Luheshi LM, *et al.* (2013) Proliferation of amyloid-beta42 aggregates occurs through a secondary nucleation mechanism. *Proc Natl Acad Sci U S A* 110(24):9758-9763.
53. Cohen SIA, Arosio P, Presto J, *et al.* (2015) A molecular chaperone breaks the catalytic cycle that generates toxic Abeta oligomers. *Nat Struct Mol Biol* 22(3):207-213.
54. Meisl G, Kirkegaard JB, Arosio P, *et al.* (2016) Molecular mechanisms of protein aggregation from global fitting of kinetic models. *Nat Protoc* 11(2):252-272.
55. Meisl G, Yang X, Dobson CM, *et al.* (2017) Modulation of electrostatic interactions to reveal a reaction network unifying the aggregation behaviour of the Abeta42 peptide and its variants. *Chem Sci* 8(6):4352-4362.
56. Scheidt T, Lapinska U, Kumita JR, *et al.* (2019) Secondary nucleation and elongation occur at different sites on Alzheimer's amyloid-beta aggregates. *Sci Adv* 5(4):9.
57. Schubert U, Anton LC, Gibbs J, *et al.* (2000) Rapid degradation of a large fraction of newly synthesized proteins by proteasomes. *Nature* 404(6779):770-774.
58. Knowles TPJ, Vendruscolo M & Dobson CM. (2014) The amyloid state and its association with protein misfolding diseases. *Nat Rev Mol Cell Biol* 15(6):384-396.
59. Westermarck P, Benson MD, Buxbaum JN, *et al.* (2007) A primer of amyloid nomenclature. *Amyloid* 14(3):179-183.
60. Winblad B, Amouyel P, Andrieu S, *et al.* (2016) Defeating Alzheimer's disease and other dementias: a priority for European science and society. *The Lancet Neurology* 15(5):455-532.
61. Alzheimer's A. (2012) 2012 Alzheimer's disease facts and figures. *Alzheimers Dement* 8(2):131-168.
62. Small GW, Rabins PV, Barry PP, *et al.* (1997) Diagnosis and treatment of Alzheimer disease and related disorders - Consensus statement of the American Association for Geriatric Psychiatry, the Alzheimer's Association, and the American Geriatrics Society. *JAMA-J Am Med Assoc* 278(16):1363-1371.
63. de Mendonca A. (2012) Rethinking Alzheimer's disease. *Front Neurol* 3:45.
64. Ballard C, Gauthier S, Corbett A, *et al.* (2011) Alzheimer's disease. *The Lancet* 377(9770):1019-1031.
65. Iadanza MG, Jackson MP, Hewitt EW, *et al.* (2018) A new era for understanding amyloid structures and disease. *Nat Rev Mol Cell Biol* 19(12):755-773.

66. Dickson DW. (1997) The pathogenesis of senile plaques. *J Neuropathol Exp Neurol* 56(4):321-339.
67. Nelson PT, Alafuzoff I, Bigio EH, *et al.* (2012) Correlation of Alzheimer disease neuropathologic changes with cognitive status: A review of the literature. *J Neuropathol Exp Neurol* 71(5):362-381.
68. Tomic JL, Pensalfini A, Head E, *et al.* (2009) Soluble fibrillar oligomer levels are elevated in Alzheimer's disease brain and correlate with cognitive dysfunction. *Neurobiol Dis* 35(3):352-358.
69. McLean CA, Cherny RA, Fraser FW, *et al.* (1999) Soluble pool of Abeta amyloid as a determinant of severity of neurodegeneration in Alzheimer's disease. *Ann Neurol* 46(6):860-866.
70. Lue LF, Kuo YM, Roher AE, *et al.* (1999) Soluble amyloid beta peptide concentration as a predictor of synaptic change in Alzheimer's disease. *Am J Pathol* 155(3):853-862.
71. Walsh DM & Selkoe DJ. (2004) Oligomers in the brain: The emerging role of soluble protein aggregates in neurodegeneration. *Protein Pept Lett* 11(3):213-228.
72. Yang T, Li S, Xu H, *et al.* (2017) Large soluble oligomers of amyloid beta-protein from Alzheimer brain are far less neuroactive than the smaller oligomers to which they dissociate. *J Neurosci* 37(1):152-163.
73. Fitzpatrick AWP, Falcon B, He S, *et al.* (2017) Cryo-EM structures of tau filaments from Alzheimer's disease. *Nature* 547(7662):185-190.
74. Vendra VP, Khan I, Chandani S, *et al.* (2016) Gamma crystallins of the human eye lens. *Biochim Biophys Acta* 1860(1 Pt B):333-343.
75. Du K, Karp PH, Ackerley C, *et al.* (2015) Aggregates of mutant CFTR fragments in airway epithelial cells of CF lungs: new pathologic observations. *J Cyst Fibros* 14(2):182-193.
76. Meng X, Clews J, Ciuta AD, *et al.* (2019) CFTR structure, stability, function and regulation. *Biol Chem* 400(10):1359-1370.
77. Albe KR, Butler MH & Wright BE. (1990) Cellular concentrations of enzymes and their substrates. *J Theor Biol* 143(2):163-195.
78. Balch WE, Morimoto RI, Dillin A, *et al.* (2008) Adapting proteostasis for disease intervention. *Science* 319(5865):916-919.
79. Hipp MS, Park SH & Hartl FU. (2014) Proteostasis impairment in protein-misfolding and -aggregation diseases. *Trends Cell Biol* 24(9):506-514.
80. Kundra R, Ciryam P, Morimoto RI, *et al.* (2017) Protein homeostasis of a metastable subproteome associated with Alzheimer's disease. *Proc Natl Acad Sci U S A* 114(28):E5703-E5711.
81. Wickner S, Maurizi MR & Gottesman S. (1999) Posttranslational quality control: Folding, refolding, and degrading proteins. *Science* 286(5446):1888-1893.

82. Kramer G, Shiber A & Bukau B. (2019) Mechanisms of Cotranslational Maturation of Newly Synthesized Proteins. In: Kornberg RD, editor. *Annual Review of Biochemistry, Vol 88*. Annual Reviews. p. 337-364.
83. Gloge F, Becker AH, Kramer G, *et al.* (2014) Co-translational mechanisms of protein maturation. *Curr Opin Struct Biol* 24:24-33.
84. Wolff S, Weissman JS & Dillin A. (2014) Differential scales of protein quality control. *Cell* 157(1):52-64.
85. Bejarano E & Cuervo AM. (2010) Chaperone-mediated autophagy. *Proc Am Thorac Soc* 7(1):29-39.
86. Kaganovich D, Kopito R & Frydman J. (2008) Misfolded proteins partition between two distinct quality control compartments. *Nature* 454(7208):1088-1095.
87. Tyedmers J, Mogk A & Bukau B. (2010) Cellular strategies for controlling protein aggregation. *Nat Rev Mol Cell Biol* 11(11):777-788.
88. Hartl FU. (1996) Molecular chaperones in cellular protein folding. *Nature* 381(6583):571-580.
89. Tissieres A, Mitchell HK & Tracy UM. (1974) Protein synthesis in salivary glands of *Drosophila melanogaster*: Relation to chromosome puffs. *J Mol Biol* 84(3):389-398.
90. Kim YE, Hipp MS, Bracher A, *et al.* (2013) Molecular chaperone functions in protein folding and proteostasis. *Annu Rev Biochem* 82:323-355.
91. Laskey RA, Honda BM, Mills AD, *et al.* (1978) Nucleosomes are assembled by an acidic protein which binds histones and transfers them to DNA. *Nature* 275(5679):416-420.
92. Ellis RJ. (2006) Molecular chaperones: assisting assembly in addition to folding. *Trends Biochem Sci* 31(7):395-401.
93. Kampinga HH, Hageman J, Vos MJ, *et al.* (2009) Guidelines for the nomenclature of the human heat shock proteins. *Cell Stress Chaperones* 14(1):105-111.
94. Frydman J, Nimmesgern E, Ohtsuka K, *et al.* (1994) Folding of nascent polypeptide-chains in a high-molecular-mass assembly with molecular chaperones. *Nature* 370(6485):111-117.
95. Haslbeck M, Franzmann T, Weinfurter D, *et al.* (2005) Some like it hot: the structure and function of small heat-shock proteins. *Nat Struct Mol Biol* 12(10):842-846.
96. Kern R, Malki A, Holmgren A, *et al.* (2003) Chaperone properties of *Escherichia coli* thioredoxin and thioredoxin reductase. *Biochem J* 371:965-972.
97. French K, Yerbury JJ & Wilson MR. (2008) Protease activation of alpha2-macroglobulin modulates a chaperone-like action with broad specificity. *Biochemistry* 47(4):1176-1185.
98. Voth W, Schick M, Gates S, *et al.* (2014) The protein targeting factor Get3 functions as ATP-independent chaperone under oxidative stress conditions. *Mol Cell* 56(1):116-127.

99. Haslbeck M, Weinkauff S & Buchner J. (2015) Regulation of the Chaperone Function of Small Hsps. In: Tanguay R, Hightower L, editors. *The Big Book on Small Heat Shock Proteins*. Springer, Cham. p. 155-178.
100. Peschek J, Braun N, Rohrberg J, *et al.* (2013) Regulated structural transitions unleash the chaperone activity of alphaB-crystallin. *Proc Natl Acad Sci U S A* 110(40):E3780-3789.
101. Benesch JLP, Ayoub M, Robinson CV, *et al.* (2008) Small heat shock protein activity is regulated by variable oligomeric substructure. *J Biol Chem* 283(42):28513-28517.
102. Ilbert M, Horst J, Ahrens S, *et al.* (2007) The redox-switch domain of Hsp33 functions as dual stress sensor. *Nat Struct Mol Biol* 14(6):556-563.
103. Quan S, Koldewey P, Tapley T, *et al.* (2011) Genetic selection designed to stabilize proteins uncovers a chaperone called Spy. *Nat Struct Mol Biol* 18(3):262-269.
104. Mchaourab HS, Godar JA & Stewart PL. (2009) Structure and mechanism of protein stability sensors: chaperone activity of small heat shock proteins. *Biochemistry* 48(18):3828-3837.
105. Fleckenstein T, Kastenmuller A, Stein ML, *et al.* (2015) The chaperone activity of the developmental small heat shock protein Sip1 is regulated by pH-dependent conformational changes. *Mol Cell* 58(6):1067-1078.
106. Haslbeck M, Walke S, Stromer T, *et al.* (1999) Hsp26: a temperature-regulated chaperone. *Embo J* 18(23):6744-6751.
107. Skouri-Panet F, Michiel M, Féraud C, *et al.* (2012) Structural and functional specificity of small heat shock protein HspB1 and HspB4, two cellular partners of HspB5: Role of the in vitro hetero-complex formation in chaperone activity. *Biochimie* 94(4):975-984.
108. Mymrikov EV, Daake M, Richter B, *et al.* (2017) The chaperone activity and substrate spectrum of human small heat shock proteins. *J Biol Chem* 292(2):672-684.
109. Suss O & Reichmann D. (2015) Protein plasticity underlines activation and function of ATP-independent chaperones. *Front Mol Biosci* 2:43.
110. Sanchez-Pulido L, Devos D & Valencia A. (2002) BRICHOS: a conserved domain in proteins associated with dementia, respiratory distress and cancer. *Trends BiochemSci* 27(7):329-332.
111. Willander H, Askarieh G, Landreh M, *et al.* (2012) High-resolution structure of a BRICHOS domain and its implications for anti-amyloid chaperone activity on lung surfactant protein C. *Proc Natl Acad Sci U S A* 109(7):2325-2329.
112. Hedlund J, Johansson J & Persson B. (2009) BRICHOS - a superfamily of multidomain proteins with diverse functions. *BMC Res Notes* 2:180.
113. Casals C, Johansson H, Saenz A, *et al.* (2008) C-terminal, endoplasmic reticulum-lumenal domain of prosurfactant protein C – structural features and membrane interactions. *FEBS J* 275(3):536-547.

114. Perez-Gil J. (2008) Structure of pulmonary surfactant membranes and films: the role of proteins and lipid-protein interactions. *Biochim Biophys Acta* 1778(7-8):1676-1695.
115. Beers MF, Kim CY, Dodia C, *et al.* (1994) Localization, synthesis, and processing of surfactant protein SP-C in rat lung analyzed by epitope-specific antipeptide antibodies. *J Biol Chem* 269(32):20318-20328.
116. Keller A, Eistetter HR, Voss T, *et al.* (1991) The pulmonary surfactant protein-C (SP-C) precursor is a type-II transmembrane protein. *Biochem J* 277:493-499.
117. Johansson J, Szyperski T & Wuthrich K. (1995) Pulmonary surfactant-associated polypeptide SP-C in lipid micelles: CD studies of intact SP-C and NMR secondary structure determination of depalmitoyl-SP-C(1-17). *FEBS Lett* 362(3):261-265.
118. Johnson AL, Braidotti P, Pietra GG, *et al.* (2001) Post-translational processing of surfactant protein-C proprotein: Targeting motifs in the NH₂-terminal flanking domain are cleaved in late compartments. *Am J Respir Cell Mol Biol* 24(3):253-263.
119. Whitsett JA & Weaver TE. (2002) Mechanisms of disease: Hydrophobic surfactant proteins in lung function and disease. *N Engl J Med* 347(26):2141-2148.
120. Vorbroker DK, Voorhout WF, Weaver TE, *et al.* (1995) Posttranslational processing of surfactant protein C in rat type II cells. *Am J Physiol-Lung Cell Mol Physiol* 269(6):L727-L733.
121. Johansson J, Szyperski T, Curstedt T, *et al.* (1994) The NMR structure of the pulmonary surfactant-associated polypeptide SP-C in an apolar solvent contains a valyl-rich alpha-helix. *Biochemistry* 33(19):6015-6023.
122. Johansson J. (1998) Structure and properties of surfactant protein C. *Biochim Biophys Acta-Mol Basis Dis* 1408(2-3):161-172.
123. Johansson J, Nerelius C, Willander H, *et al.* (2010) Conformational preferences of non-polar amino acid residues: an additional factor in amyloid formation. *Biochem Biophys Res Commun* 402(3):515-518.
124. Kallberg Y, Gustafsson M, Persson B, *et al.* (2001) Prediction of amyloid fibril-forming proteins. *J Biol Chem* 276(16):12945-12950.
125. Nogee LM, Dunbar AE, Wert SE, *et al.* (2001) A mutation in the surfactant protein C gene associated with familial interstitial lung disease. *N Engl J Med* 344(8):573-579.
126. Nogee LM, Dunbar AE, Wert S, *et al.* (2002) Mutations in the surfactant protein C gene associated with interstitial lung disease. *Chest* 121(3):20S-21S.
127. Willander H, Hermansson E, Johansson J, *et al.* (2011) BRICHOS domain associated with lung fibrosis, dementia and cancer – a chaperone that prevents amyloid fibril formation? *FEBS J* 278(20):3893-3904.
128. Beers MF, Lomax CA & Russo SJ. (1998) Synthetic processing of surfactant protein C by alveolar epithelial cells: The COOH terminus of proSP-C is required for post-translational targeting and proteolysis. *J Biol Chem* 273(24):15287-15293.

129. Conkright JJ, Na CL & Weaver TE. (2002) Overexpression of surfactant protein-C mature peptide causes neonatal lethality in transgenic mice. *Am J Respir Cell Mol Biol* 26(1):85-90.
130. Vidal R, Frangione B, Rostagno A, *et al.* (1999) A stop-codon mutation in the BRI gene associated with familial British dementia. *Nature* 399(6738):776-781.
131. Buxbaum JN & Johansson J. (2017) Transthyretin and BRICHOS: The paradox of amyloidogenic proteins with anti-amyloidogenic activity for abeta in the central nervous system. *Front Neurosci* 11:119.
132. Kim SH, Wang R, Gordon DJ, *et al.* (1999) Furin mediates enhanced production of fibrillogenic ABri peptides in familial British dementia. *Nat Neurosci* 2(11):984-988.
133. Matsuda S, Matsuda Y, Snapp EL, *et al.* (2011) Maturation of BRI2 generates a specific inhibitor that reduces APP processing at the plasma membrane and in endocytic vesicles. *Neurobiol Aging* 32(8):1400-1408.
134. Kim SH, Creemers JW, Chu S, *et al.* (2002) Proteolytic processing of familial British dementia-associated BRI variants: Evidence for enhanced intracellular accumulation of amyloidogenic peptides. *J Biol Chem* 277(3):1872-1877.
135. Martin L, Fluhrer R, Reiss K, *et al.* (2008) Regulated intramembrane proteolysis of Bri2 (Itm2b) by ADAM10 and SPPL2a/SPPL2b. *J Biol Chem* 283(3):1644-1652.
136. Sisodia SS. (1992) Beta-amyloid precursor protein cleavage by a membrane-bound protease. *Proc Natl Acad Sci U S A* 89(13):6075-6079.
137. Vidal R, Revesz T, Rostagno A, *et al.* (2000) A decamer duplication in the 3' region of the BRI gene originates an amyloid peptide that is associated with dementia in a Danish kindred. *Proc Natl Acad Sci U S A* 97(9):4920-4925.
138. Mead S, James-Galton M, Revesz T, *et al.* (2000) Familial British dementia with amyloid angiopathy: Early clinical, neuropsychological and imaging findings. *Brain* 123:975-991.
139. Cantlon A, Frigerio CS & Walsh DM. (2015) Lessons from a rare familial dementia: Amyloid and beyond. *J Parkinsons Dis Alzheimers Dis* 2(1).
140. Deleersnijder W, Hong GZ, Cortvrindt R, *et al.* (1996) Isolation of markers for chondro-osteogenic differentiation using cDNA library subtraction: Molecular cloning and characterization of a gene belonging to a novel multigene family of integral membrane proteins. *J Biol Chem* 271(32):19475-19482.
141. Van den Plas D & Merregaert J. (2004) In vitro studies on Itm2a reveal its involvement in early stages of the chondrogenic differentiation pathway. *Biol Cell* 96(6):463-470.
142. Kihara M, Kiyoshima T, Nagata K, *et al.* (2014) Itm2a expression in the developing mouse first lower molar, and the subcellular localization of Itm2a in mouse dental epithelial cells. *Plos One* 9(7):11.
143. Martin L, Fluhrer R & Haass C. (2009) Substrate requirements for SPPL2b-dependent regulated intramembrane proteolysis. *J Biol Chem* 284(9):5662-5670.

144. Vidal R, Calero M, Revesz T, *et al.* (2001) Sequence, genomic structure and tissue expression of Human BRI3, a member of the BRI gene family. *Gene* 266(1-2):95-102.
145. Matsuda S, Matsuda Y & D'Adamio L. (2009) BRI3 inhibits Amyloid Precursor Protein Processing in a mechanistically distinct manner from its homologue dementia gene BRI2. *J Biol Chem* 284(23):15815-15825.
146. Dai J, Zhang N, Wang JH, *et al.* (2014) Gastrokine-2 is downregulated in gastric cancer and its restoration suppresses gastric tumorigenesis and cancer metastasis. *Tumor Biol* 35(5):4199-4207.
147. Oien KA, McGregor F, Butler S, *et al.* (2004) Gastrokine 1 is abundantly and specifically expressed in superficial gastric epithelium, down-regulated in gastric carcinoma, and shows high evolutionary conservation. *J Pathol* 203(3):789-797.
148. Altieri F, Di Stadio CS, Severino V, *et al.* (2014) Anti-amyloidogenic property of human gastrokine 1. *Biochimie* 106:91-100.
149. Menheniott TR, Peterson AJ, O'Connor L, *et al.* (2010) A novel gastrokine, Gkn3, marks gastric atrophy and shows evidence of adaptive gene loss in humans. *Gastroenterology* 138(5):1823-1835.
150. Hayami T, Shukunami C, Mitsui K, *et al.* (1999) Specific loss of chondromodulin-I gene expression in chondrosarcoma and the suppression of tumor angiogenesis and growth by its recombinant protein in vivo. *FEBS Lett* 458(3):436-440.
151. Zhu SP, Qiu H, Bennett S, *et al.* (2019) Chondromodulin-1 in health, osteoarthritis, cancer, and heart disease. *Cell Mol Life Sci* 76(22):4493-4502.
152. Shukunami C, Takimoto A, Miura S, *et al.* (2008) Chondromodulin-I and tenomodulin are differentially expressed in the avascular mesenchyme during mouse and chick development. *Cell Tissue Res* 332(1):111-122.
153. Oshima Y, Sato K, Tashiro F, *et al.* (2004) Anti-angiogenic action of the C-terminal domain of tenomodulin that shares homology with chondromodulin-I. *J Cell Sci* 117(13):2731-2744.
154. Bruno R, Maresca M, Canaan S, *et al.* (2019) Worms' Antimicrobial Peptides. *Mar Drugs* 17(9):22.
155. Knight SD, Presto J, Linse S, *et al.* (2013) The BRICHOS domain, amyloid fibril formation, and their relationship. *Biochemistry* 52(43):7523-7531.
156. Fitzen M, Alvelius G, Nordling K, *et al.* (2009) Peptide-binding specificity of the prosurfactant protein C Brichos domain analyzed by electrospray ionization mass spectrometry. *Rapid Commun Mass Spectrom* 23(22):3591-3598.
157. Biverstål H, Dolfe L, Hermansson E, *et al.* (2015) Dissociation of a BRICHOS trimer into monomers leads to increased inhibitory effect on Aβ42 fibril formation. *Biochim Biophys Acta* 1854(8):835-843.
158. Yang J, Yan R, Roy A, *et al.* (2015) The I-TASSER Suite: protein structure and function prediction. *Nat Methods* 12(1):7-8.

159. Hermansson E, Schultz S, Crowther D, *et al.* (2014) The chaperone domain BRICHOS prevents CNS toxicity of amyloid-beta peptide in *Drosophila melanogaster*. *Dis Model Mech* 7(6):659-665.
160. Arosio P, Michaels TC, Linse S, *et al.* (2016) Kinetic analysis reveals the diversity of microscopic mechanisms through which molecular chaperones suppress amyloid formation. *Nat Commun* 7:10948.
161. Poska H, Haslbeck M, Kurudenkandy FR, *et al.* (2016) Dementia-related Bri2 BRICHOS is a versatile molecular chaperone that efficiently inhibits Abeta42 toxicity in *Drosophila*. *Biochem J* 473(20):3683-3704.
162. Willander H, Presto J, Askarieh G, *et al.* (2012) BRICHOS domains efficiently delay fibrillation of amyloid beta-peptide. *J Biol Chem* 287(37):31608-31617.
163. Nerelius C, Gustafsson M, Nordling K, *et al.* (2009) Anti-amyloid activity of the C-terminal domain of proSP-C against amyloid beta-peptide and medin. *Biochemistry* 48(17):3778-3786.
164. Peng S, Fitzen M, Jornvall H, *et al.* (2010) The extracellular domain of Bri2 (ITM2B) binds the ABri peptide (1-23) and amyloid beta-peptide (Abeta1-40): Implications for Bri2 effects on processing of amyloid precursor protein and Abeta aggregation. *Biochem Biophys Res Commun* 393(3):356-361.
165. Kurudenkandy FR, Zilberter M, Biverstal H, *et al.* (2014) Amyloid-beta-induced action potential desynchronization and degradation of hippocampal gamma oscillations is prevented by interference with peptide conformation change and aggregation. *J Neurosci* 34(34):11416-11425.
166. Whitmore L & Wallace BA. (2008) Protein secondary structure analyses from circular dichroism spectroscopy: Methods and reference databases. *Biopolymers* 89(5):392-400.
167. Ho CS, Lam CWK, Chan MHM, *et al.* (2003) Electrospray Ionisation Mass Spectrometry: Principles and Clinical Applications. *Clin Biochem Rev* 24(1):3-12.
168. Lakowicz RJ. (2006) *Principles of Fluorescence Spectroscopy*. 3rd edition ed: Springer Science & Business Media, LLC.
169. Hawe A, Sutter M & Jiskoot W. (2008) Extrinsic fluorescent dyes as tools for protein characterization. *Pharm Res* 25(7):1487-1499.
170. Biancalana M & Koide S. (2010) Molecular mechanism of Thioflavin-T binding to amyloid fibrils. *Biochim Biophys Acta* 1804(7):1405-1412.
171. Flagmeier P, De SM, Michaels TCT, *et al.* (2020) Direct measurement of lipid membrane disruption connects kinetics and toxicity of Abeta 42 aggregation. *Nat Struct Mol Biol*:18.
172. Aprile FA, Sormanni P, Perni M, *et al.* (2017) Selective targeting of primary and secondary nucleation pathways in A beta 42 aggregation using a rational antibody scanning method. *Sci Adv* 3(6):11.

173. Limbocker R, Chia S, Ruggeri FS, *et al.* (2019) Trodusquemine enhances Abeta42 aggregation but suppresses its toxicity by displacing oligomers from cell membranes. *Nat Commun* 10(1):225.
174. Krichevsky O & Bonnet G. (2002) Fluorescence correlation spectroscopy: the technique and its applications. *Rep Prog Phys* 65(2):251-297.
175. Macháň R & Hof M. Practical manual for fluorescence microscopy techniques; Chapert 5: Fluorescence Correlation Spectroscopy (FCS). Picoquant; 2016.
176. Elson EL & Magde D. (1974) Fluorescence correlation spectroscopy. I. conceptual basis and theory. *Biopolymers* 13(1):1-27.
177. Sengupta P, Garai K, Balaji J, *et al.* (2003) Measuring size distribution in highly heterogeneous systems with fluorescence correlation spectroscopy. *Biophys J* 84(3):1977-1984.
178. Sun GY, Guo SM, Teh C, *et al.* (2015) Bayesian model selection applied to the analysis of Fluorescence Correlation Spectroscopy data of fluorescent proteins in vitro and in vivo. *Anal Chem* 87(8):4326-4333.
179. Kronqvist N, Sarr M, Lindqvist A, *et al.* (2017) Efficient protein production inspired by how spiders make silk. *Nat Commun* 8:15504.
180. Basha E, Jones C, Blackwell AE, *et al.* (2013) An unusual dimeric small heat shock protein provides insight into the mechanism of this class of chaperones. *J Mol Biol* 425(10):1683-1696.
181. Delbecq SP & Klevit RE. (2013) One size does not fit all: the oligomeric states of alphaB crystallin. *FEBS Lett* 587(8):1073-1080.
182. Basha E, O'Neill H & Vierling E. (2012) Small heat shock proteins and alpha-crystallins: dynamic proteins with flexible functions. *Trends BiochemSci* 37(3):106-117.
183. Haslbeck M & Vierling E. (2015) A first line of stress defense: small heat shock proteins and their function in protein homeostasis. *J Mol Biol* 427(7):1537-1548.
184. Iaccarino HF, Singer AC, Martorell AJ, *et al.* (2018) Gamma frequency entrainment attenuates amyloid load and modifies microglia. *Nature* 562(7725):230-235.
185. Ribary U, Ioannides AA, Singh KD, *et al.* (1991) Magnetic-field tomography of coherent thalamocortical 40-Hz oscillations in humans. *Proc Natl Acad Sci U S A* 88(24):11037-11041.
186. Yamamoto J, Suh J, Takeuchi D, *et al.* (2014) Successful execution of working memory linked to synchronized high-frequency gamma oscillations. *Cell* 157(4):845-857.
187. Wälti MA, Ravotti F, Arai H, *et al.* (2016) Atomic-resolution structure of a disease-relevant Abeta(1-42) amyloid fibril. *Proc Natl Acad Sci U S A* 113(34):E4976-E4984.
188. Colvin MT, Silvers R, Ni QZ, *et al.* (2016) Atomic resolution structure of monomorphic Abeta(42) amyloid fibrils. *J Am Chem Soc* 138(30):9663-9674.

189. Jang HH, Lee KO, Chi YH, *et al.* (2004) Two enzymes in one; two yeast peroxiredoxins display oxidative stress-dependent switching from a peroxidase to a molecular chaperone function. *Cell* 117(5):625-635.
190. Yi MC & Khosla C. (2016) Thiol-disulfide exchange reactions in the mammalian extracellular environment. In: Prausnitz JM, editor. *Annual Review of Chemical and Biomolecular Engineering, Vol 7*. Annual Reviews. p. 197-222.
191. Badia MC, Giraldo E, Dasi F, *et al.* (2013) Reductive stress in young healthy individuals at risk of Alzheimer disease. *Free Radic Biol Med* 63:274-279.
192. Perez-Torres I, Guarner-Lans V & Rubio-Ruiz ME. (2017) Reductive stress in inflammation-associated diseases and the pro-oxidant effect of antioxidant agents. *Int J Mol Sci* 18(10).
193. Brewer AC, Mustafi SB, Murray TV, *et al.* (2013) Reductive stress linked to small HSPs, G6PD, and Nrf2 pathways in heart disease. *Antioxid Redox Signal* 18(9):1114-1127.
194. Michaels TCT, Saric A, Curk S, *et al.* (2020) Dynamics of oligomer populations formed during the aggregation of Alzheimer's Abeta 42 peptide. *Nat Chem* 12(5):445-451.
195. Törnquist M, Cukalevski R, Weininger U, *et al.* (2020) Ultrastructural evidence for self-replication of Alzheimer-associated Abeta42 amyloid along the sides of fibrils. *Proc Natl Acad Sci U S A* 117(21):11265-11273.
196. Linse S, Scheidt T, Bernfur K, *et al.* (2020) Kinetic fingerprints differentiate the mechanisms of action of anti-Abeta antibodies. *Nat Struct Mol Biol*.
197. Fabrizi C, Businaro R, Lauro GM, *et al.* (2001) Role of alpha(2)-macroglobulin in regulating amyloid beta-protein neurotoxicity: protective or detrimental factor? *J Neurochem* 78(2):406-412.
198. Hammad SM, Ranganathan S, Loukinova E, *et al.* (1997) Interaction of apolipoprotein J-amyloid beta-peptide complex with low density lipoprotein receptor-related protein-2 megalin: A mechanism to prevent pathological accumulation of amyloid beta-peptide. *J Biol Chem* 272(30):18644-18649.
199. Galan-Acosta L, Sierra C, Leppert A, *et al.* (2020) Recombinant BRICHOS chaperone domains delivered to mouse brain parenchyma by focused ultrasound and microbubbles are internalized by hippocampal and cortical neurons. *Mol Cell Neurosci* 105:103498.